Electronic Supplementary Material (ESI) for Chemical Communications.

Zwitterionic BODIPYs with Larger Stokes Shift: Small Molecular Biomarkers for Live Cells

Adiki Raja Sekhar,[a] Santhosh Kumar Sariki,[b] R. V. Ramana Reddy,[a] Alakesh Bisai,[a] Pushpendra Kumar Sahu,[b] Raghuvir Singh Tomar,[b] Jeyaraman Sankar*[a]

[a] Department of Chemistry, Indian Institute of Science Education and Research Bhopal, Bhopal bypass road, Bhouri, Bhopal, India-462066. Fax: +91-755-6692392; Tel: +91-755-6692334.

[b] Laboratory of Chromatin Biology, Department of Biological Sciences, Indian Institute of Science Education and Research Bhopal, Bhopal bypass road, Bhouri, Bhopal, India-462066. Fax: +91-755-6692392; Tel: +91-755-6692334.

Supporting Information

1. General Information

All solvents and reagents were purchased from commercial sources and used without further purification except for dry THF which was further distilled over sodium metal. Mass spectra were recorded on a Bruker HR-LCMS spectrometer using CH_3OH and $CHCl_3$ as solvents. 100 MHz for ^{13}C, 376 MHz for ^{19}F, 128 MHz for ^{11}B and 500 MHz for ^{1}H- NMR spectra were recorded using a Bruker instrument operating at 500 MHz in deuterated solvent of methanol and dimethyl sulfoxide solvent. UV/Vis spectra were recorded on Cary-100 spectrophotometry. Fluorescence emission spectra were recorded on a Horiba Jovin Vyon Fluoro log 3-111 spectrophotometer.

UV/Vis and fluorescence experiments were carried with stock solution of Zwitterionic BODIPY **2** and **3** and diluted in cuvette for further analysis, prepared in methanol (HPLC grade). Absorption coefficient of zwitterionic BODIPYs was calculated in same solvent. In fluorescence, BODIPYs was excited at λ_{max} with entrance and exit slits 1 nm and 1 nm respectively. Experiments were carried under ambient conditions. Quantum yields of BODIPYs compounds were calculated with respect to coumarin 153 (Φ=0.58) in ethanol. **2** and **3** were excited at cross point with standard sample in absorption profile. Quantum yield was calculated according to the following formula

$$\Phi_X = \Phi_R[\frac{A_R(\lambda_r)}{A_X(\lambda_x)}][\frac{I(\lambda_r)}{I(\lambda_x)}][\frac{\eta_x^2}{\eta_r^2}][\frac{D_x}{D_r}]$$

where I(λr) is the Relative Intensity of the existing light at wavelength λ, η is the average refractive index of the solution, D is the area under the emission spectrum, A(λ) is the absorbance per cm of the solution at the excitation wavelength λ. Subscripts "x" and "r" refer to the unknown and reference solutions, respectively. Since the solvent used is the same for both the unknown and the reference, hence it is assumed that I(λx)= I(λr). Then the equation is further simplified as:

$$\Phi_X = \Phi_R[\frac{A_R(\lambda_r)}{A_X(\lambda_x)}][\frac{D_x}{D_r}]$$

Single crystal data was collected on a Bruker APEX II diffractometer equipped with a graphite monochromator and Mo-Kα (λ = 0.71073 Å) radiation. Data collection was performed using φ and ω scans. The structures was solved using direct method followed by full matrix least square refinements against F2 (all data HKLF 4 format) using SHELXTL.[1] Subsequent difference Fourier synthesis and least-square refinement revealed the positions of the remaining non-hydrogen atoms. Determinations of the crystal system, orientation matrix, and cell dimensions were performed according to the established procedures. Lorentz polarization and multi-scan absorption correction were applied. Non-hydrogen atoms were refined with independent anisotropic displacement parameters and hydrogen atoms were placed geometrically and refined using the riding model. All calculations were carried out using SHELXL[2] and WinGXsystemVer-1.6414.

2. Synthetic procedure

2 ml of trimethylamine in water was added to the solution of dibromo-pentafluorophenyl BODIPY 100 mg in 20 ml of dry chloroform. The reaction mixture was stirred for 24 h at room temperature in an open atmospheric condition. Concentrate the reaction mixture under reduced pressure, to remove an inseparable mixture subjected to neutral alumina column chromatography in ethyl acetate without any further extraction. Purified desire compounds by slow increment of polarity in neutral alumina column chromatography. By gradual increment in polarity from Hexane, ethyl acetate to methanol afforded pure product of Oxo and Imino- BODIPYs. By repetitive precipitation in ethyl acetate gives dry powder of desired products.

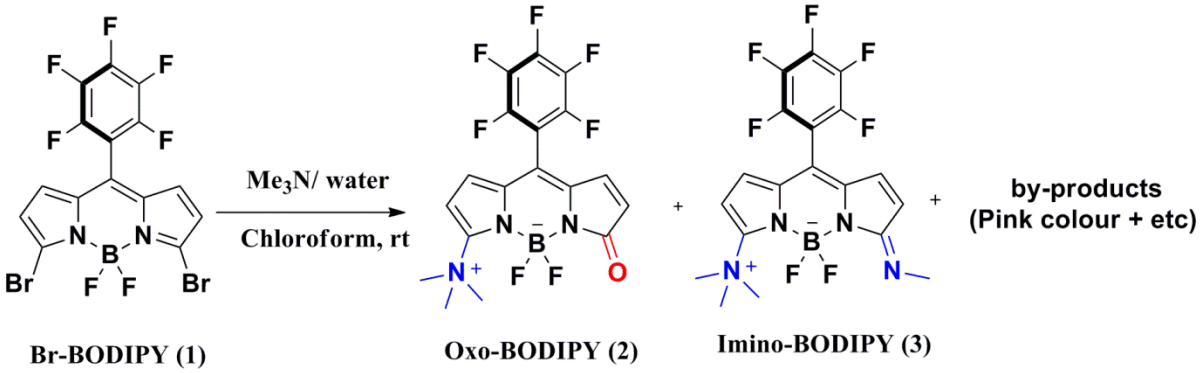

Scheme S1. Synthesis procedure of Zwitterionic BODIPYs

Oxo-BODIPY (2):

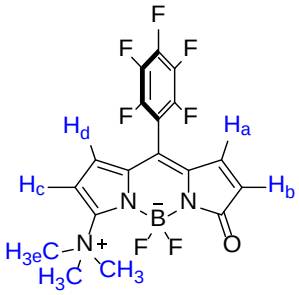

Oxo⁻BODIPY (2)

Light green shining solid in 30 mg (35.9 % yield). ^{1}H NMR ($(CD_3)_2SO$, 500 MHz): δ (ppm) 7.09-7.08 (d, 1H_a, *J*= 5.34 Hz), 6.46-6.45 (d, 1H_c, *J*= 4.18 Hz), 6.14-6.13 (d, 1H_b, *J*= 5.34 Hz), 5.90-5.89 (d, 1H_d, *J*= 4.18 Hz), 3.71 (s, 9H_e); ^{13}C NMR ($(CD_3)_2SO$, 125 MHz): δ (ppm) 173.94, 146.12, 144. 76, 141.88, 139.91, 138.37, 137.10, 134.51, 133.19, 126.74, 109.52, 107.55, 105.32, 98.57, 57.65-57.59; ^{19}F ($(CD_3)_2SO$, 470 MHz): -δ (ppm) 130.33-130.42, 140.00-140.07, 155.22-155.31, 162.21-162.33; ^{11}B ($(CD_3)_2SO$, 160 MHz) δ (ppm) 0.44 (t, $J_{B\text{-}F}$ = 30.17 Hz). HR-MS (ESI): m/z calc for $C_{18}H_{13}BF_7N_3ONa$ 454.0935, found 454.0962. UV/Vis (CH_3OH): λ (nm) - 390 (2.258×10^4 M^{-1} cm^{-1}) and 405 (2.178×10^4 M^{-1} cm^{-1}). Emission (excitation at 390 nm): λ_{emi} = 461 nm.

Imino-BODIPY (3):

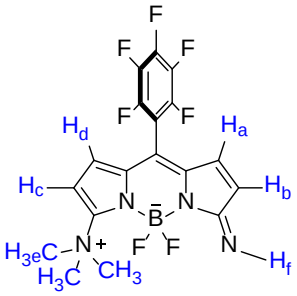

Imino-BODIPY (3)

Dark green solid in 20 mg (23.27 % yield). ^{1}H NMR (CD_3OD, 500 MHz): δ (ppm) 7.25-7.24 (d, 1H_a, *J*= 4.88 Hz), 6.96-6.95 (d, 1H_b, *J*= 5.05 Hz), 6.65-6.64 (d, 1H_c, *J*= 3.35 Hz), 6.24-6.23 (d, 1H_d, *J*= 3.35 Hz), 3.85 (s, 9H_e), 3.28 (s, 3H_f); ^{13}C NMR (CD_3OD, 125 MHz): δ (ppm) 172.02, 164.85, 145.62, 144.34,141.96, 138.42,137.78, 136.92, 135.72, 132.56, 118.56, 113.38, 109.87, 107.72, 106.12, 57.32, 30.68; ^{19}F (CD_3OD, 470 MHz): -δ (ppm) 136.73-136.96, 141.13-141.18, 154.63-154.72, 163.50-163.60; ^{11}B (CD_3OD, 160 MHz) δ (ppm) 1.55-1.11 (t, J_{B-F}= 35.43 Hz). HR-MS (ESI): m/z calc for $C_{19}H_{16}BF_7N_4$ + H 445.1432, found 445.1439. UV/Vis (Methanol): λ (nm) - 414 (1.84×10^4 M^{-1} cm^{-1}); 434 (1.982×10^4 M^{-1} cm^{-1}). Emission (excitation at 410 nm): λ_{emi}= 406 nm.

3. Photophysical properties

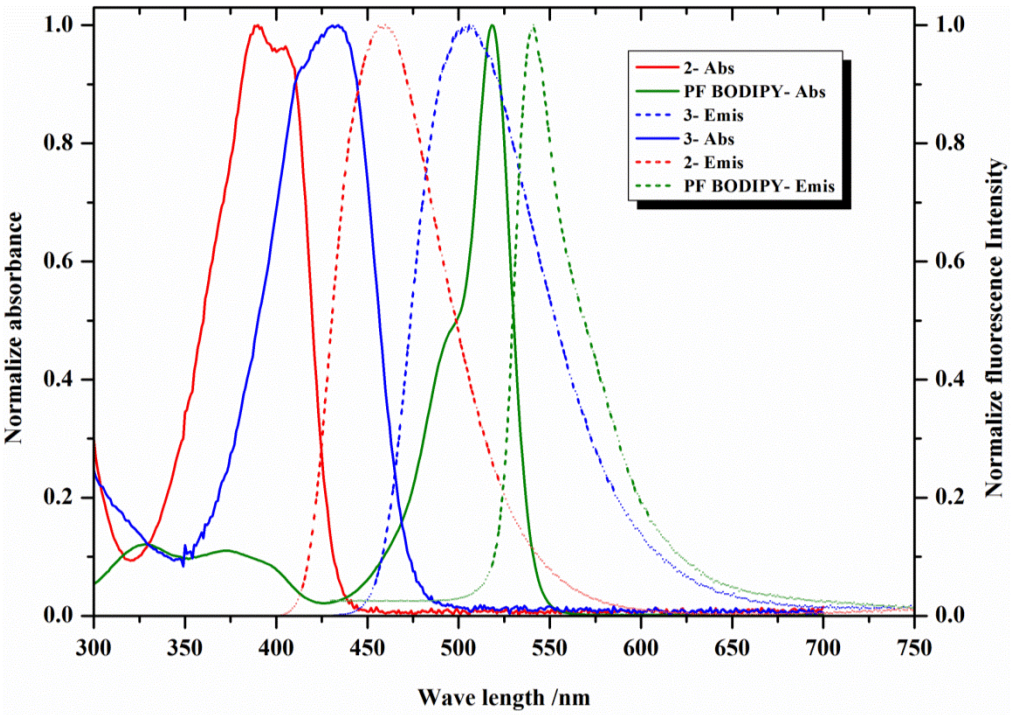

Figure S1. Comparision photophysical properties of Oxo-BODIPY (**2**) and Imino BODIPY (**3**) with typical PF BODIPY in DCM.

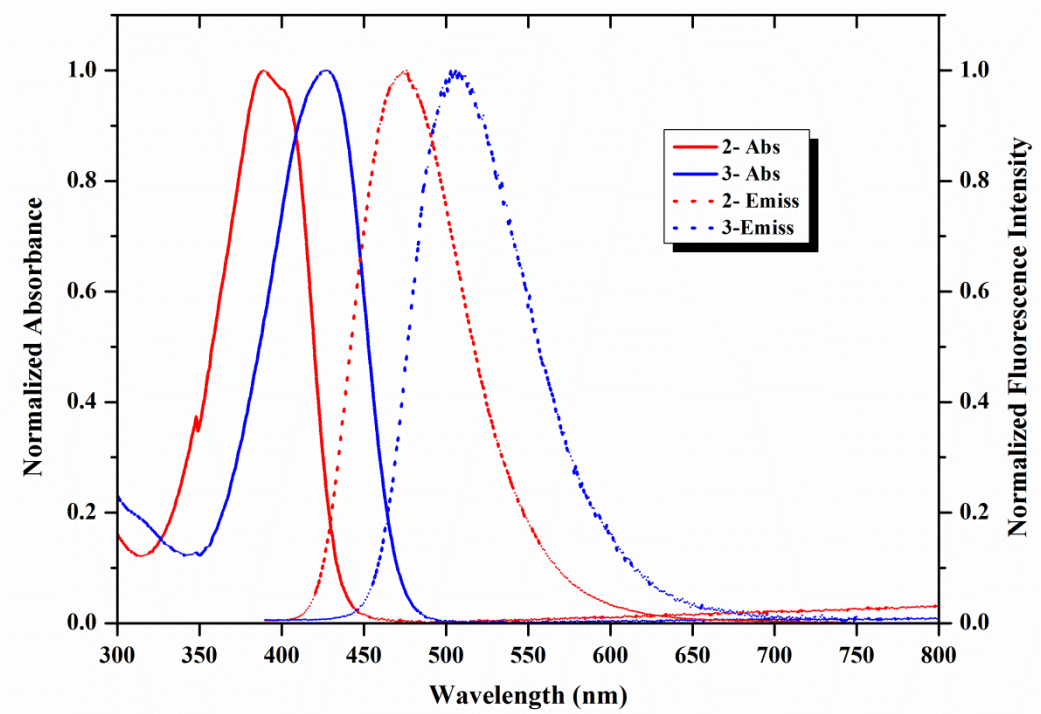

Figure S2. Photophysical properties of Oxo-BODIPY (**2**) and Imino BODIPY (**3**) in PBS buffer (pH-7).

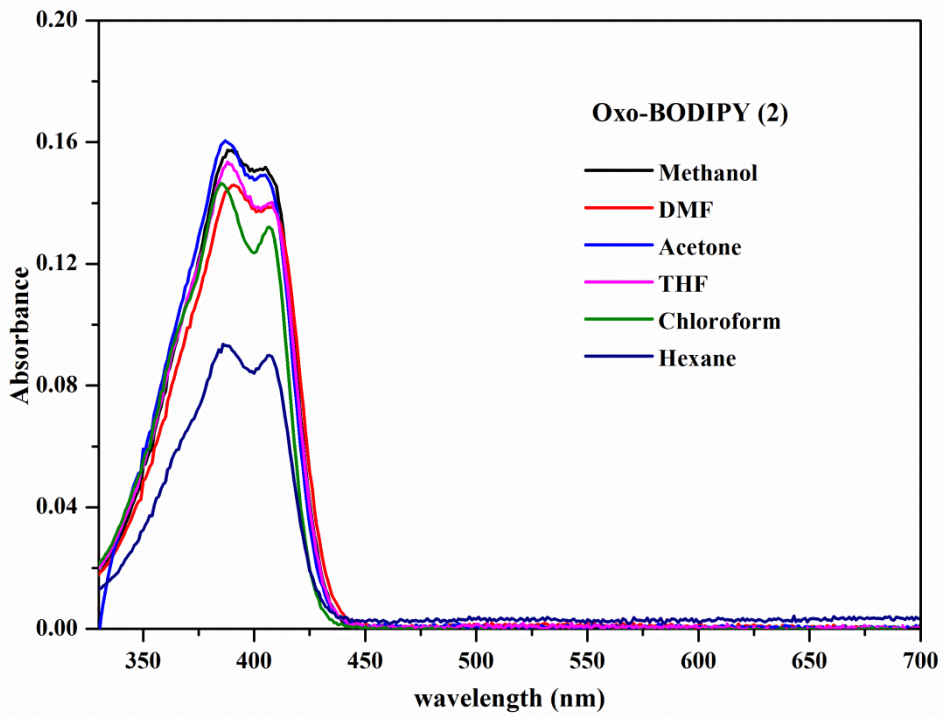

Figure S3. Absorption spectra of Oxo-BODIPY (**2**) in different solvents.

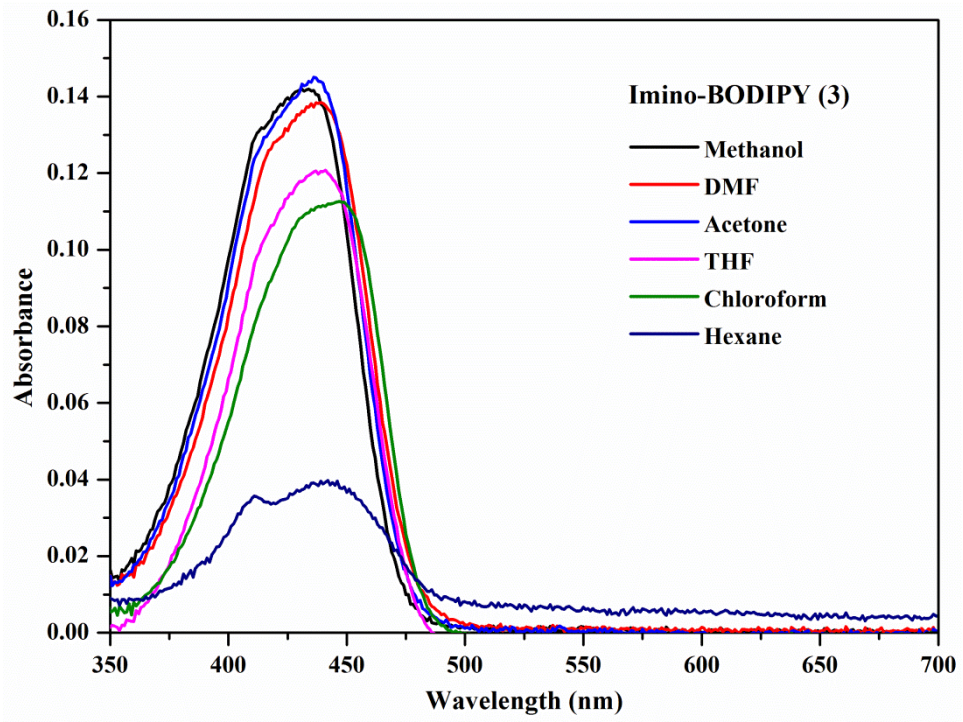

Figure S4. Absorption spectra of Imino-BODIPY (**3**) in different solvents.

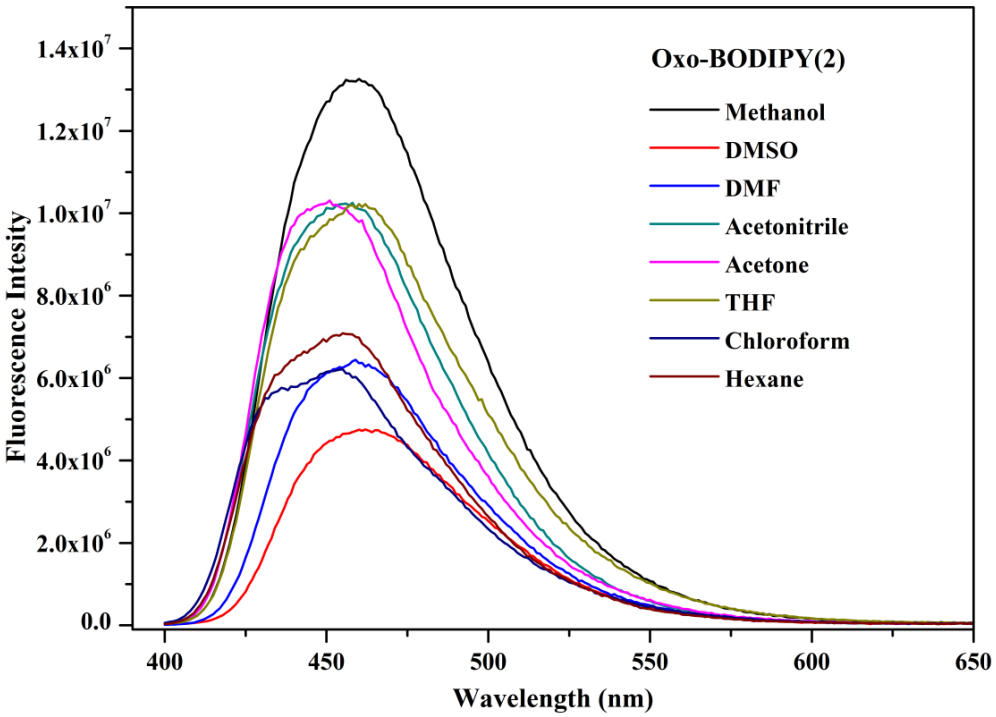

Figure S5. Fluorescence spectra of Oxo-BODIPY (**2**) in different solvents.

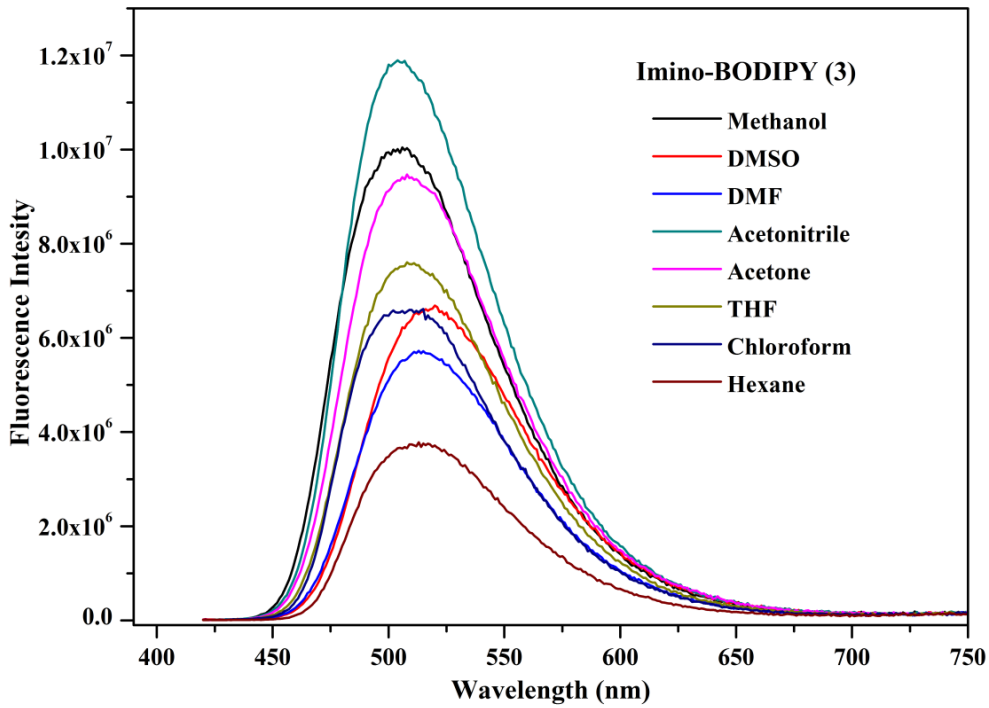

Figure S6. Fluorescence spectra of Imino-BODIPY (**3**) in different solvents.

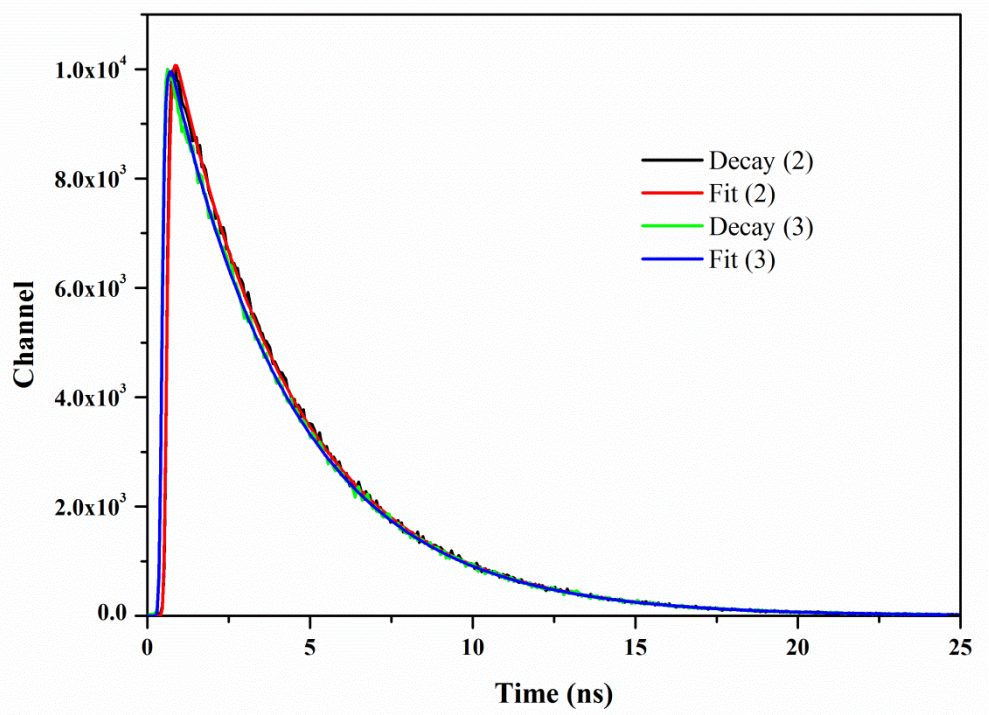

Figure S7. Fluorescence lifetime of Oxo-BODIPY (**2**) and Imino-BODIPY (**3**) in methanol solvents.

4. NMR and Mass spectra.

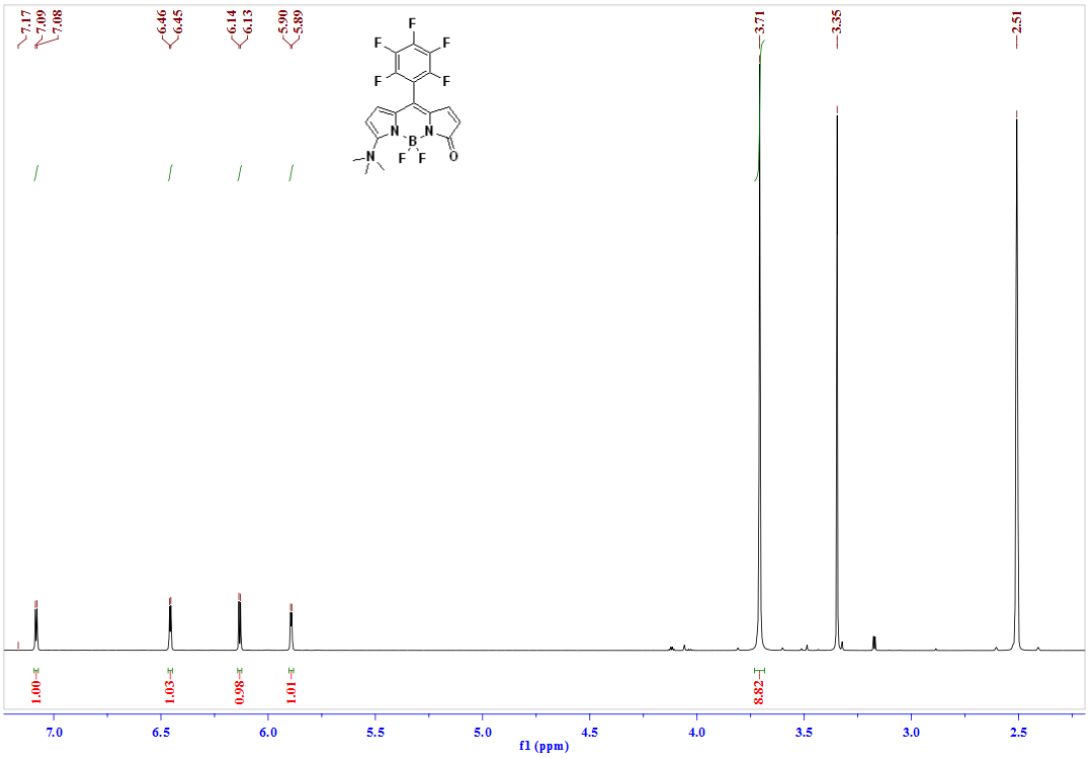

Figure S8. ^{1}H- NMR spectrum of Oxo-BODIPY (**2**) in DMSO- D_6 solvent.

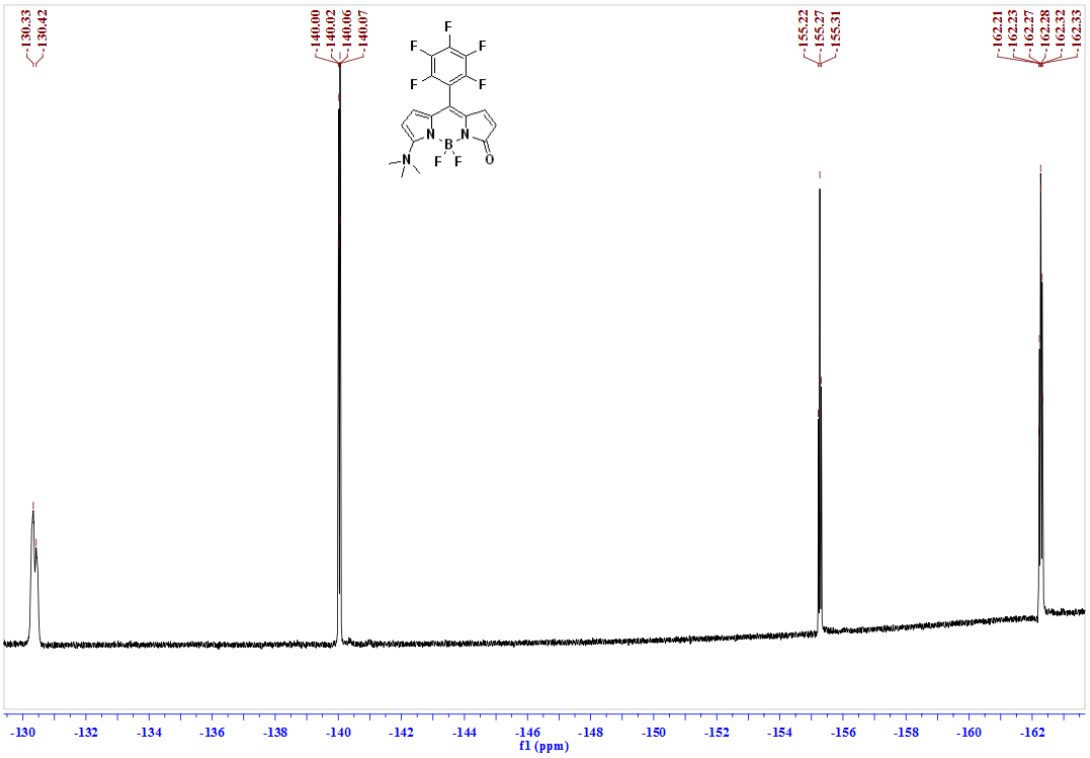

Figure S9. ^{19}F- NMR spectrum of Oxo-BODIPY (**2**) in DMSO- D_6 solvent.

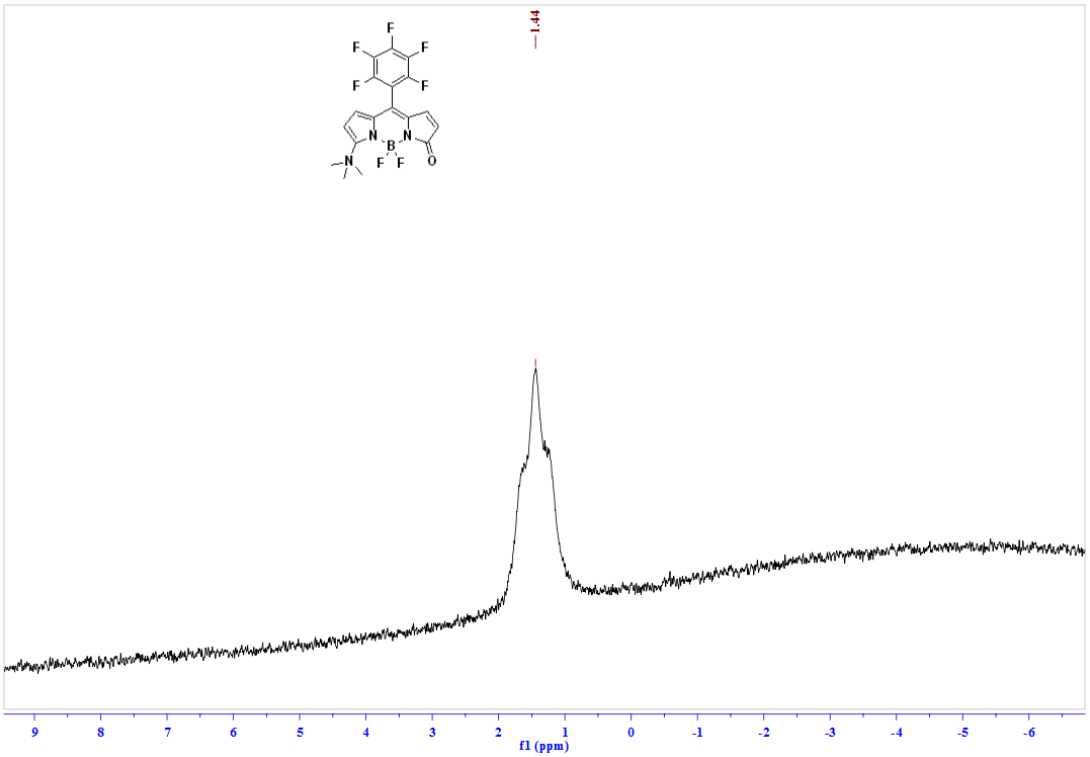

Figure S10. ^{11}B- NMR spectrum of Oxo-BODIPY (**2**) in DMSO- D_6 solvent.

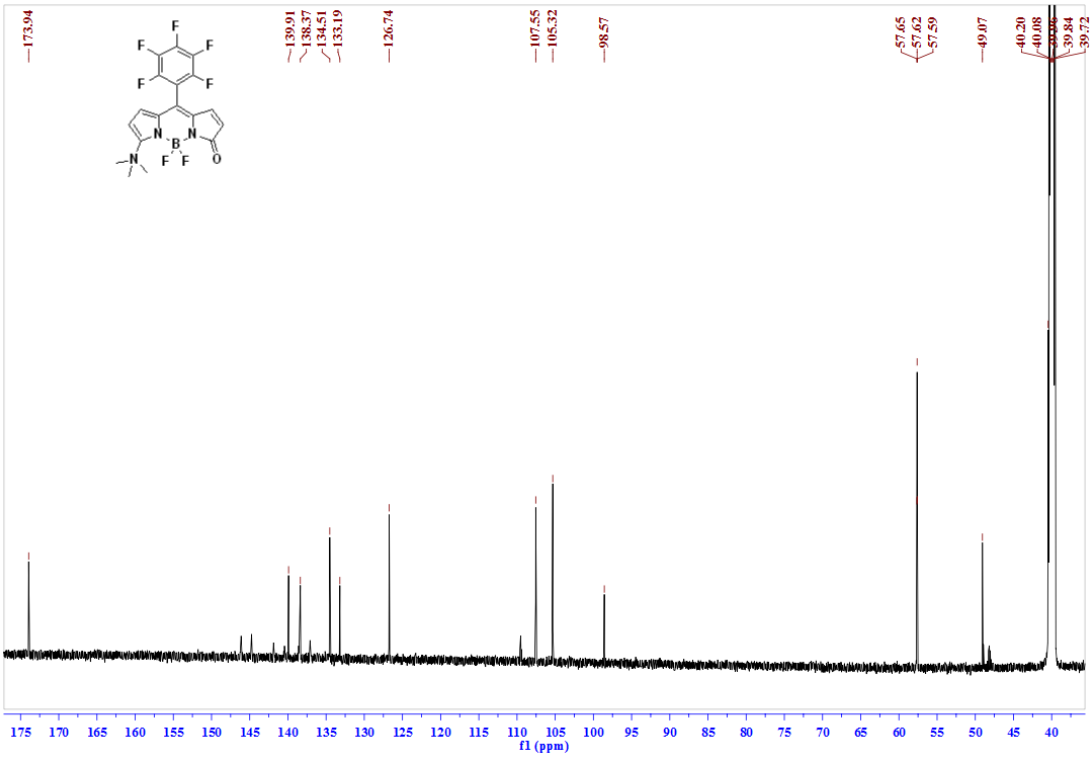

Figure S11. ^{13}C- NMR spectrum of Oxo-BODIPY (**2**) in DMSO- D_6 solvent.

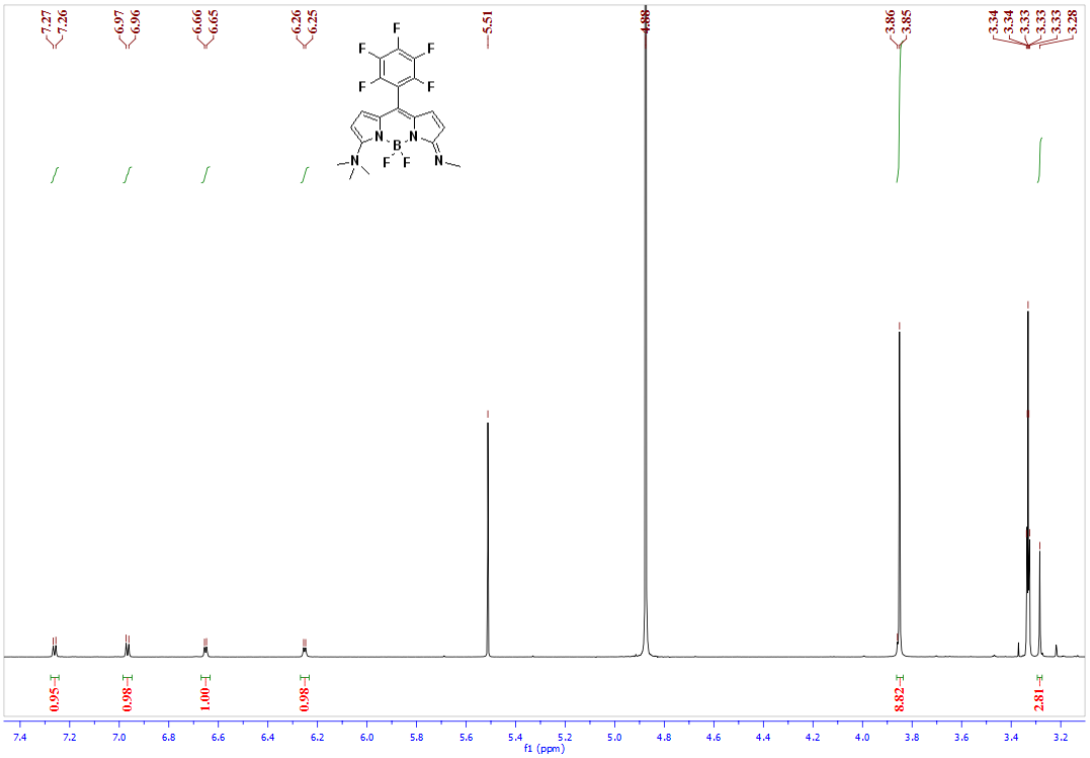

Figure S12. ^{1}H- NMR spectrum of Imino-BODIPY (**3**) in CD_3OD solvent.

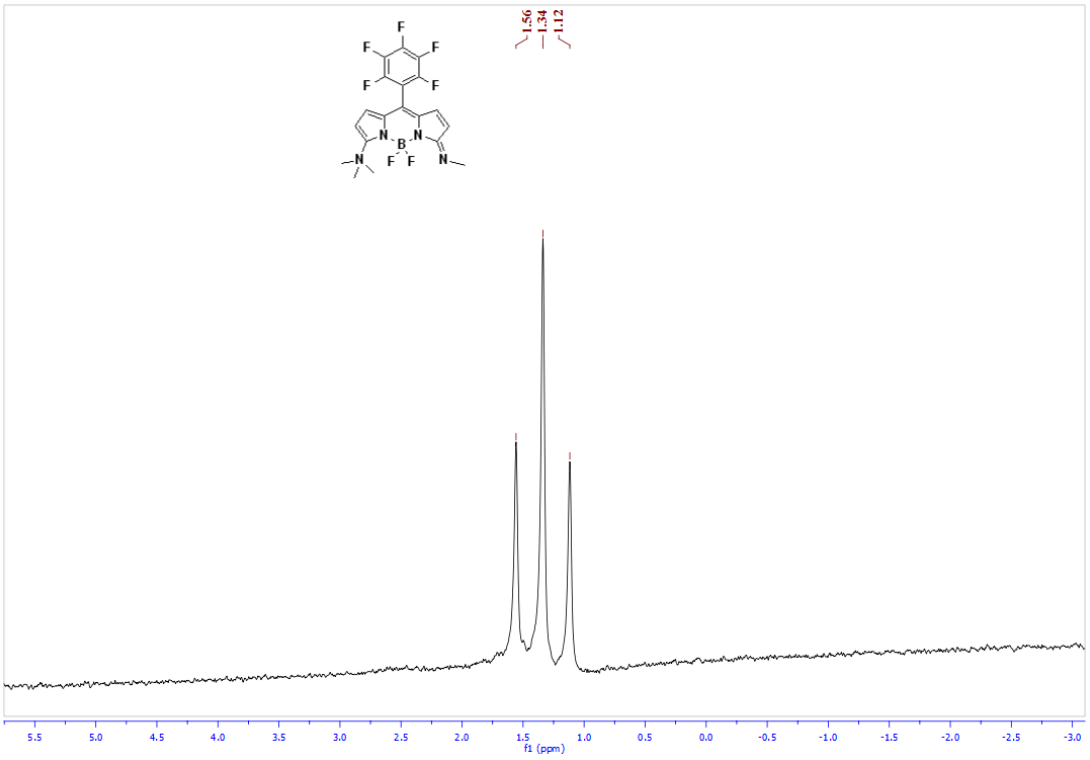

Figure S13. ^{11}B- NMR spectrum of Imino-BODIPY (**3**) in CD_3OD solvent.

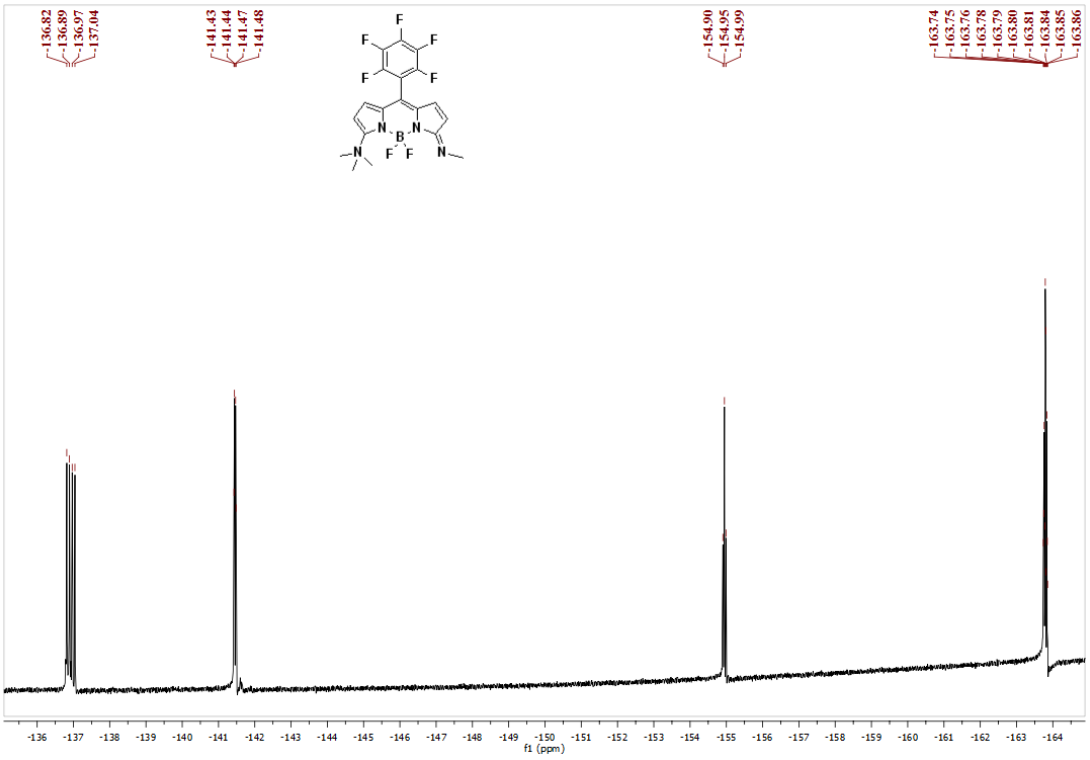

Figure S14. ^{19}F- NMR spectrum of Imino-BODIPY (**3**) in CD_3OD solvent.

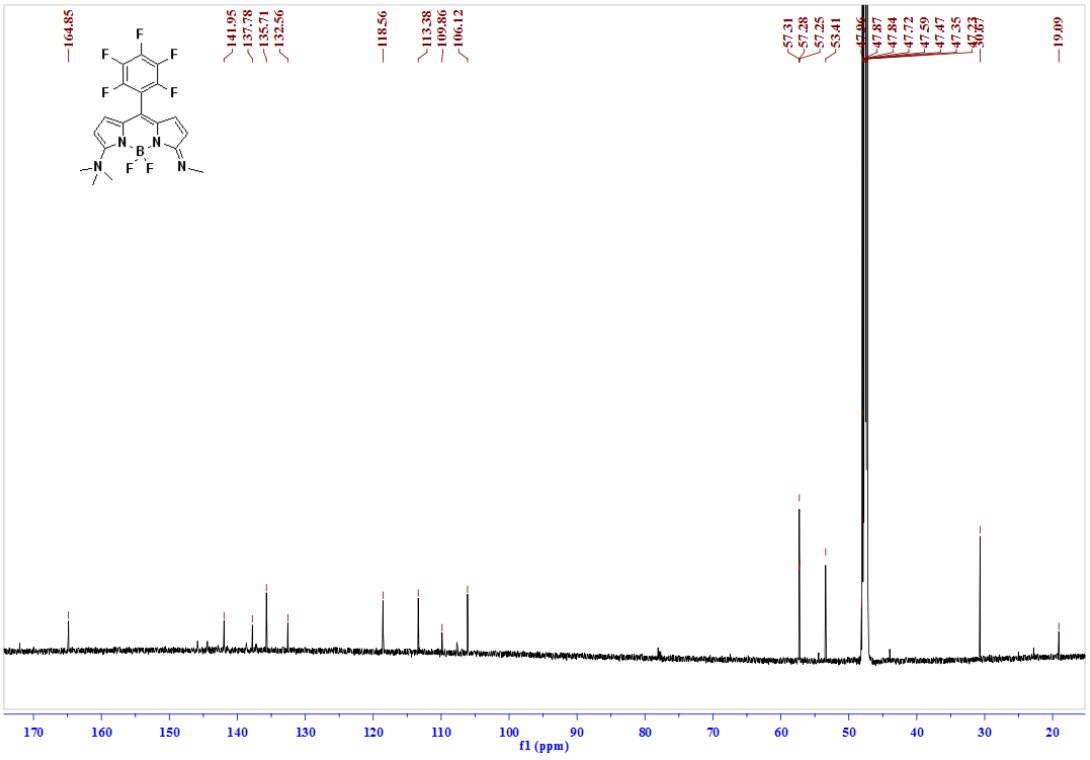

Figure S15. ^{13}C- NMR spectrum of Imino-BODIPY (**3**) in CD_3OD solvent.

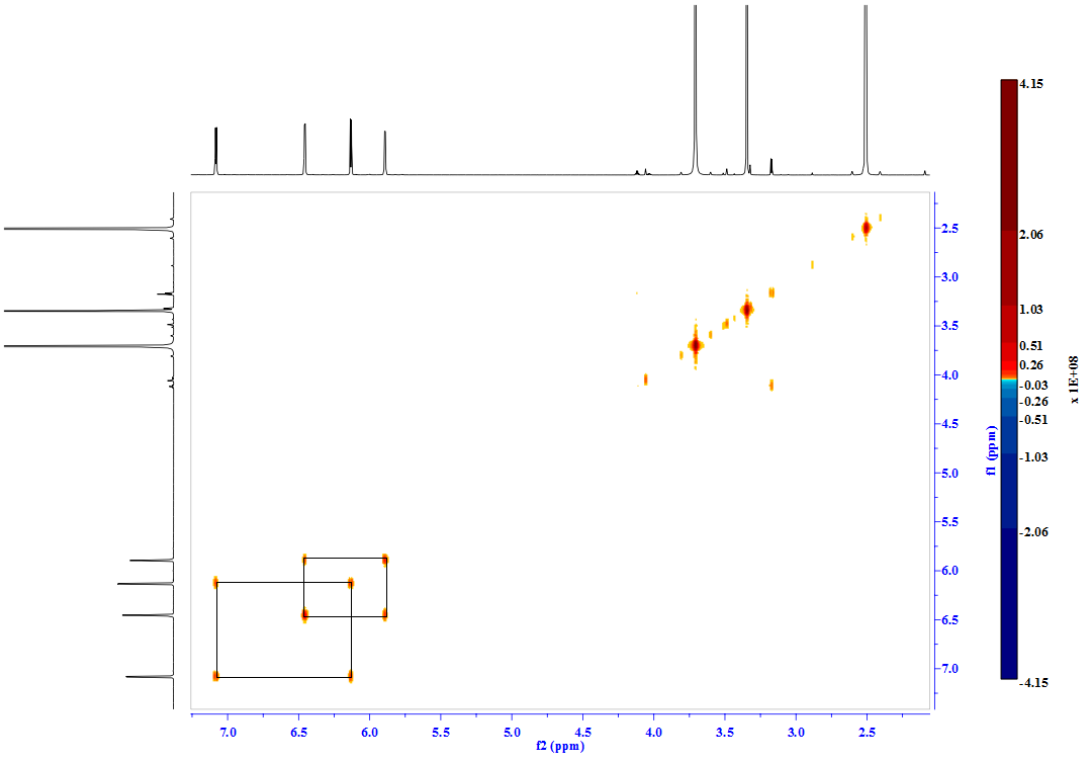

Figure S16. COSY- NMR spectrum of Oxo-BODIPY (**2**) in DMSO- D_6 solvent.

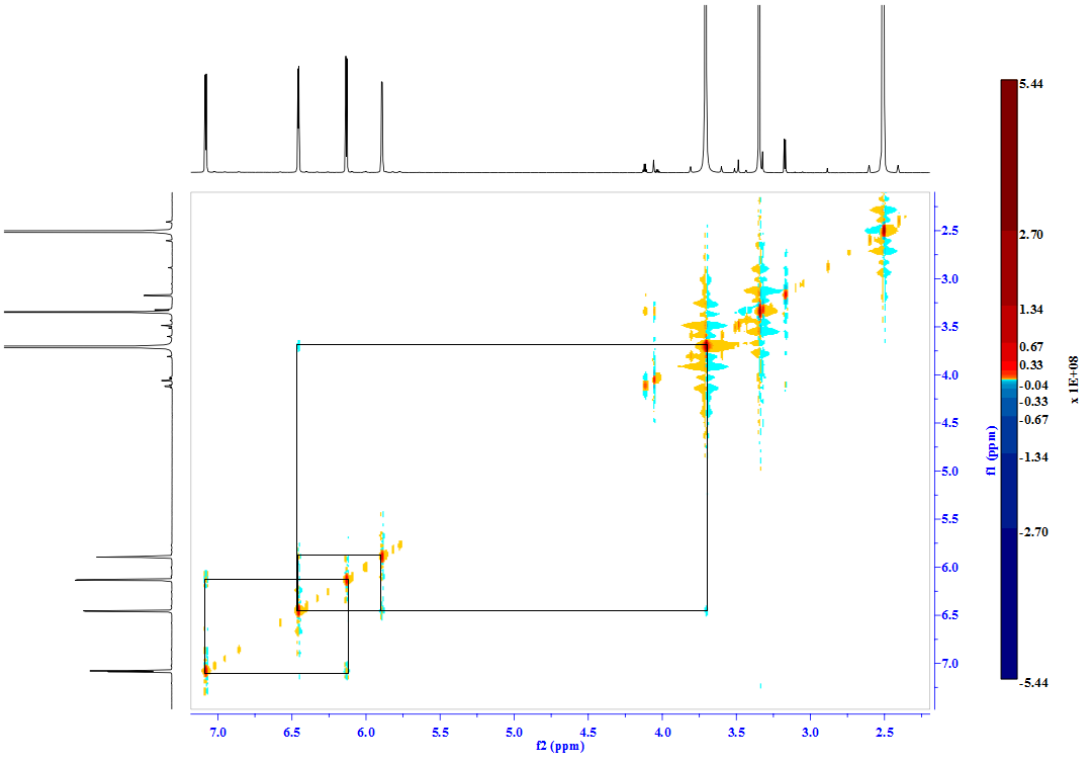

Figure S17. NOSY- NMR spectrum of Oxo-BODIPY (**2**) in DMSO- D_6 solvent.

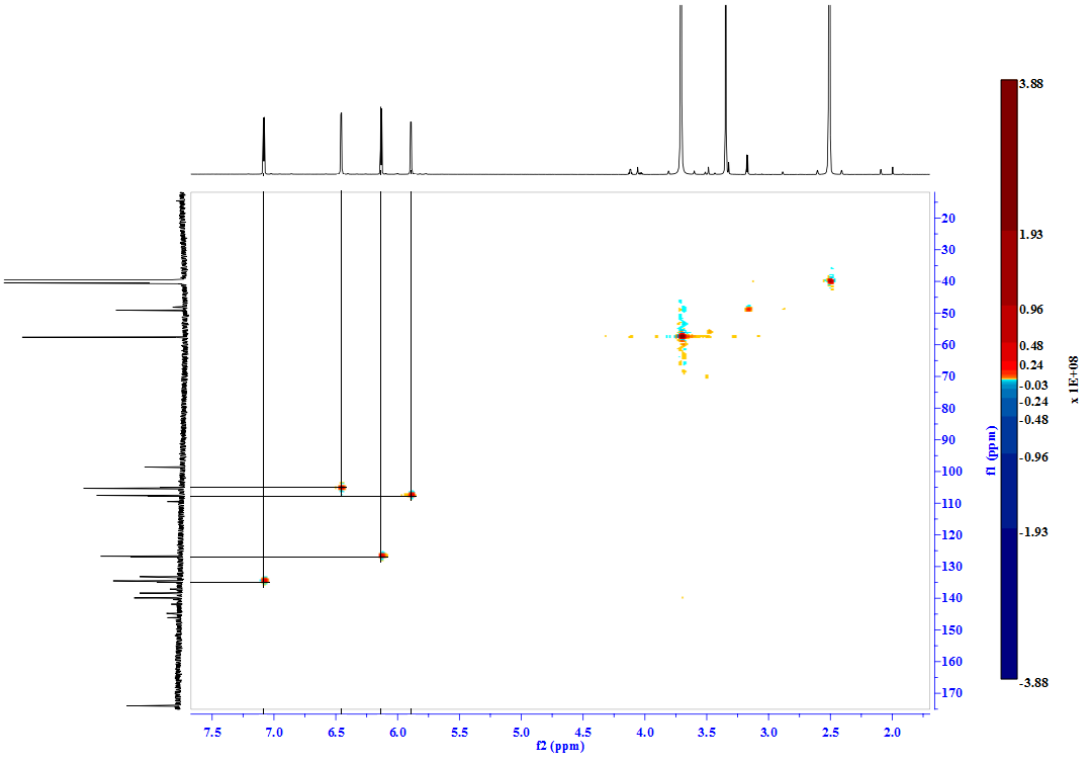

Figure S18. HSQC- NMR spectrum of Oxo-BODIPY (**2**) in DMSO- D_6 solvent.

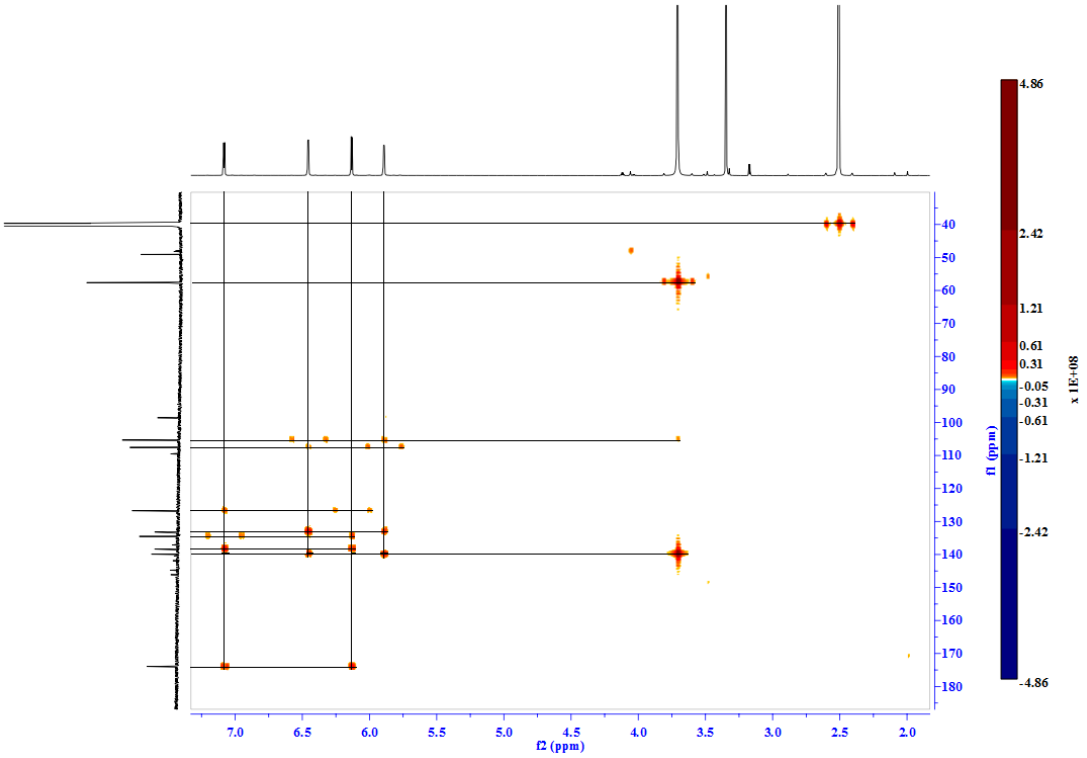

Figure S19. HMBC- NMR spectrum of Oxo-BODIPY (**2**) in DMSO- D_6 solvent.

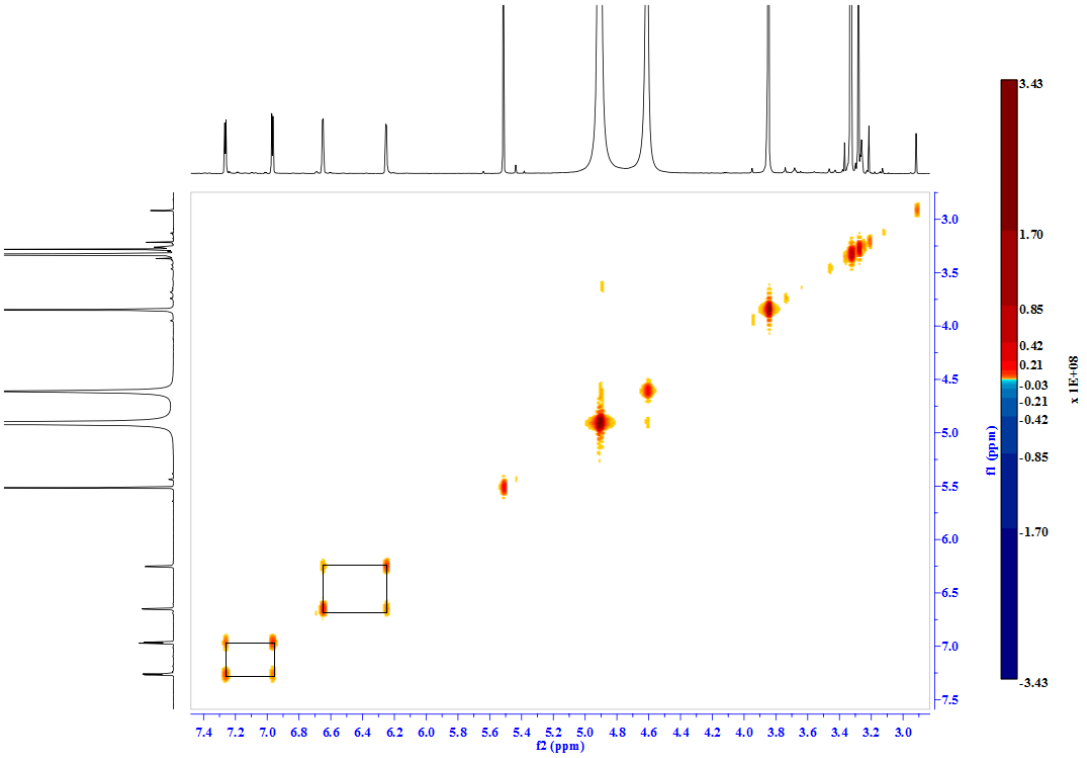

Figure S20. COSY- NMR spectrum of Imino-BODIPY (**3**) in CD_3OD solvent.

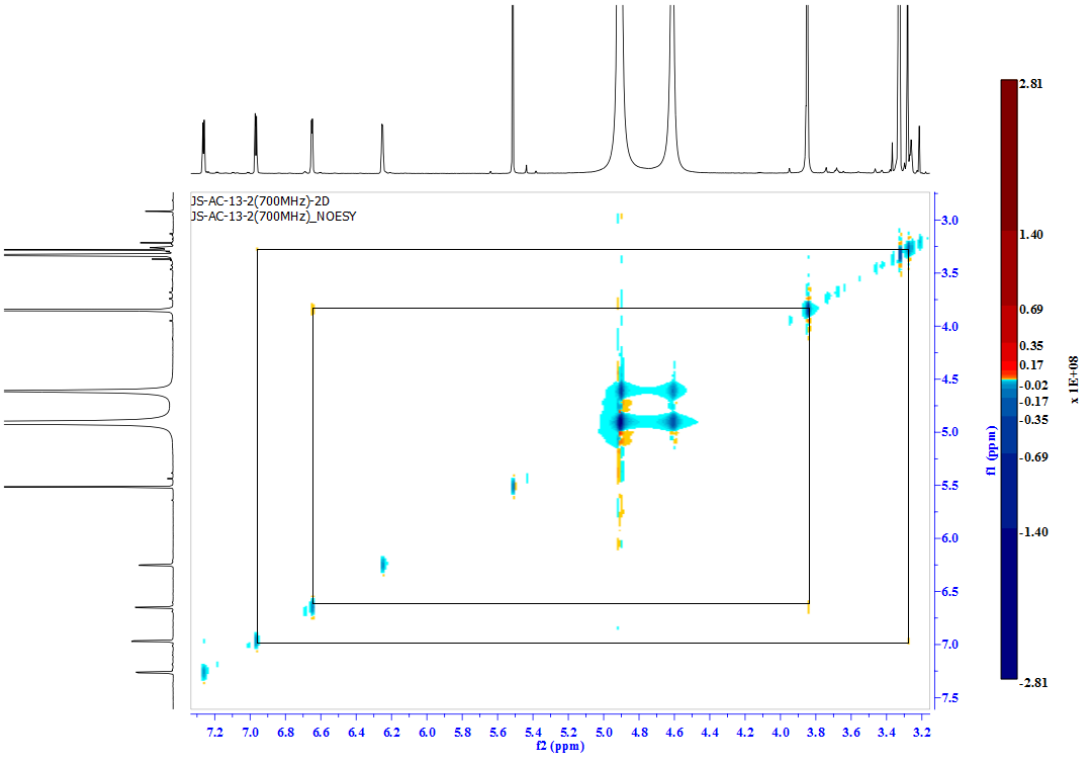

Figure S21. NOSY- NMR spectrum of Imino-BODIPY (**3**) in CD_3OD solvent.

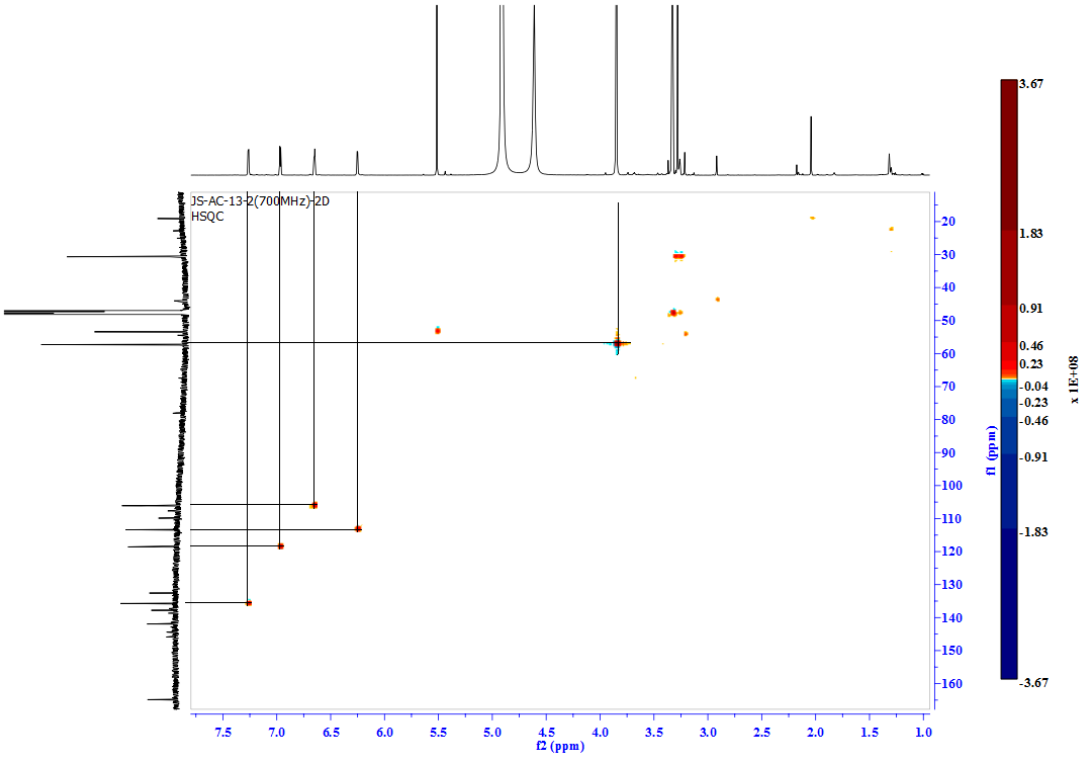

Figure S22. HSQC- NMR spectrum of Imino-BODIPY (**3**) in CD_3OD solvent.

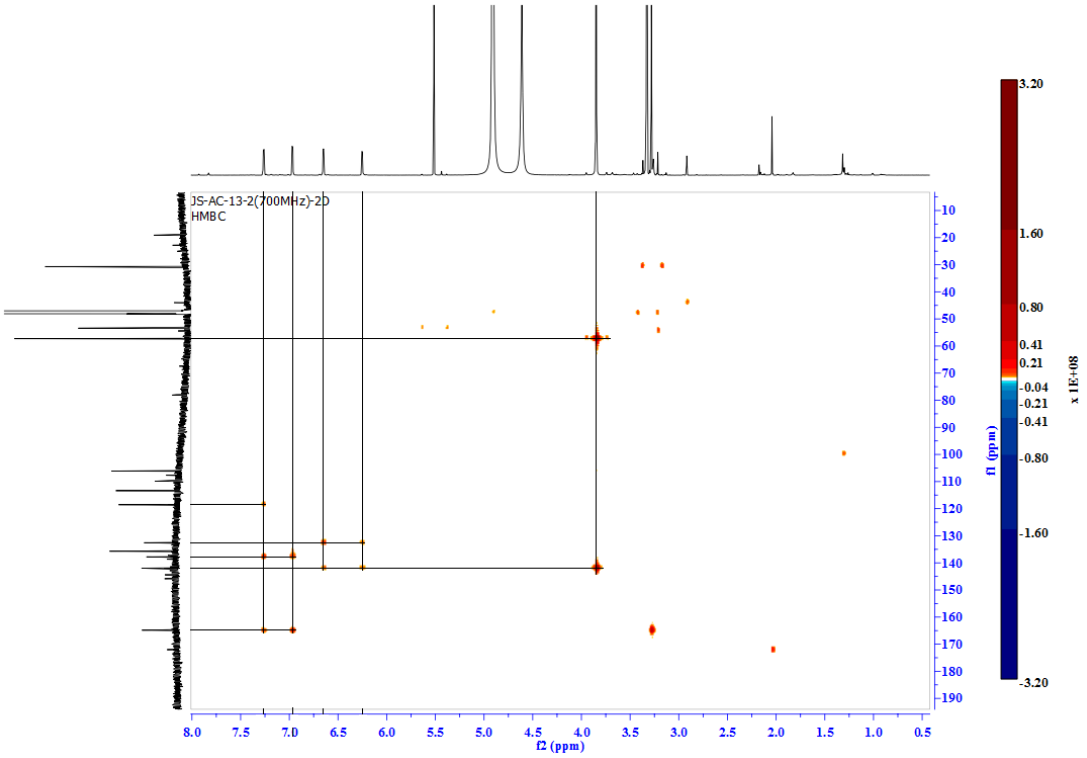

Figure S23. HMBC- NMR spectrum of Imino-BODIPY (**3**) in CD_3ODs solvent.

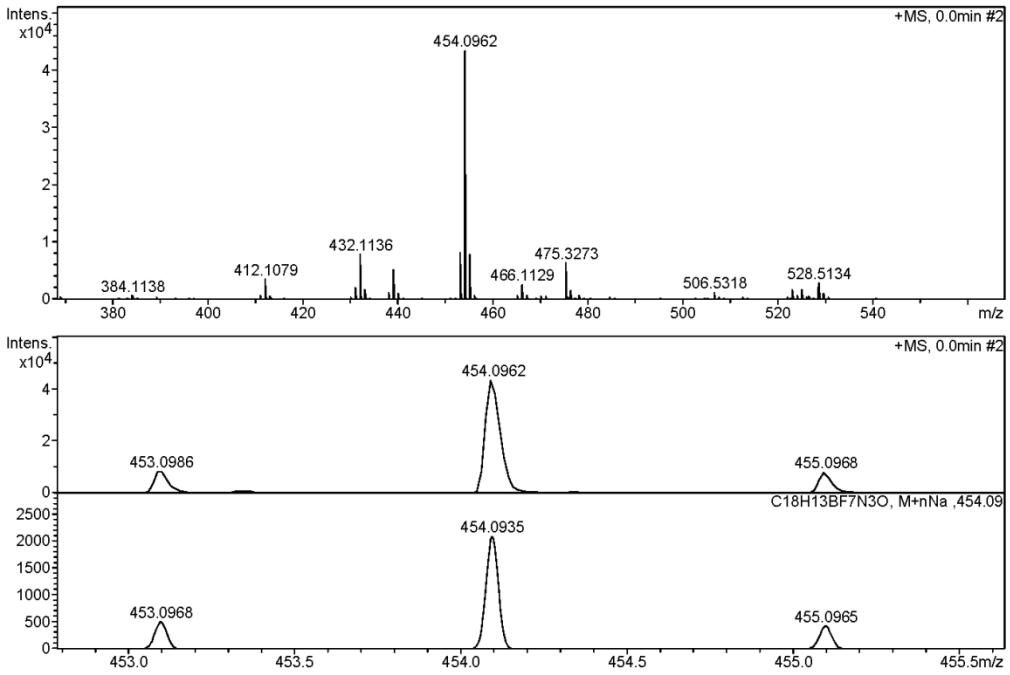

Figure S24. HR-MS of Oxo-BODIPY (**2**) in methanol solvent.

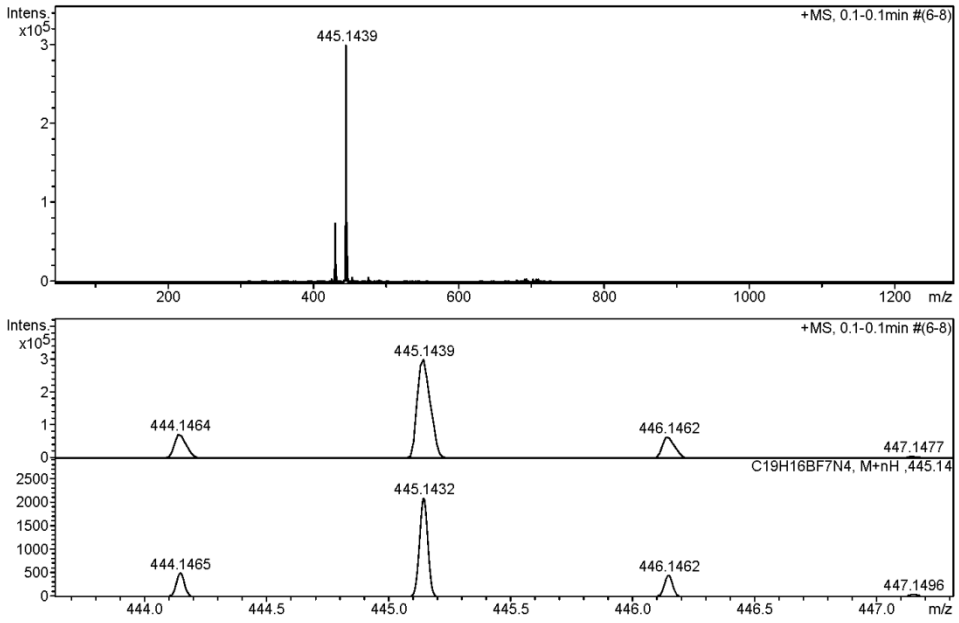

Figure S25. HR-MS of Imino-BODIPY (**3**) in methanol solvent.

5. Geometrical Calculation

a. Distortion Angular index (τ_4)

Angular index (**τ4**) is a measurement to describe distortion in tetrahedral geometry, which is proposed by Robert P. Houser and co-workers is

$$\tau_4 = \frac{360° - (\alpha + \beta)}{141°}$$

α and β are two largest angle in tetrahedral geometry of boron. According to angular index, the value range from 0 (square planar) to 1 (tetrahedral).

Geometry	τ_4
Tetrahedral (T_d)	1.00
Trigonal pyramidal (C_{3v})	0.85
Seesaw (C_{2v}, θ_6 = 90◦)	0.64
Seesaw (C_{2v}, θ_6 = 109.5◦)	0.50
Seesaw (C_{2v}, θ_6 = 154.4◦)	0.18
Seesaw (C_{2v}, θ_6 = 170◦)	0.07
Square planar (D_{4h})	0.00

Table S1. Four-coordinate geometry indices for ideal geometrical shapes

b. Donor –Acceptor Tetrahedral Calculation (THC_{D-A})

The geometry of four coordination boron systems and to know the strength of coordination covalent bond Herbert Hopfl proposed tetrahedral donor-acceptor equation for B-N system is

$$\boldsymbol{THC_{D-A}}(\%) = \left[\mathbf{1} - \frac{\sum_{n=1-6}|\mathbf{109.5} - \boldsymbol{\theta_n}|}{\mathbf{3(120-109.5)°-3(109.5-90)°}}\right] \times \mathbf{100}$$

After generalized the formula

$$\boldsymbol{THC_{D-A}}(\%) = \left[\mathbf{1} - \frac{\sum_{n=1-6}|\mathbf{109.5} - \boldsymbol{\theta_n}|}{\mathbf{90°}}\right] \times \mathbf{100}$$

Where θ= angle in tetrahedral geometry around boron atom.

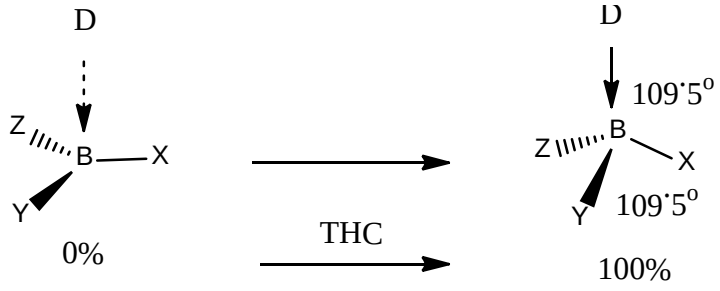

Compound	Structure	*d* (N→.B) (Å)	THC_{D-A} (%)
α-BN	Hexagonal	3.33	0
β-BN	Cubic	1.57	100

Table S2. Tetrahedral character calculation of four-coordinate geometry for ideal geometrical shapes

Atom 1	Atom 2	d 1,2 [Å]	Atom 3	d 1,3 [Å]	Angle 2,1,3 [°]

B1	F2	1.3808	F1	1.4046	110.262
B1	F2	1.3808	N1	1.5265	110.030
B1	F2	1.3808	N2	1.5797	111.613
B1	F1	1.4046	N1	1.5265	110.452
B1	F1	1.4046	N2	1.5797	107.604
B1	N1	1.5265	N2	1.5797	106.803

Table S3. Bond angles and distance of boron coordinate geometry in Oxo-BODIPY (**2**)

Atom 1	Atom 2	d 1,2 [Å]	Atom 3	d 1,3 [Å]	Angle 2,1,3 [°]
B1	F2	1.3749	F1	1.3998	109.270
B1	F2	1.3749	N1	1.5029	111.667
B1	F2	1.3749	N2	1.5798	109.630
B1	F1	1.3998	N1	1.5029	110.450
B1	F1	1.3998	N2	1.5798	107.389
B1	N1	1.5029	N2	1.5798	108.334

Table S4. Bond angles and distance of boron coordinate geometry in Imino-BODIPY (**3**)

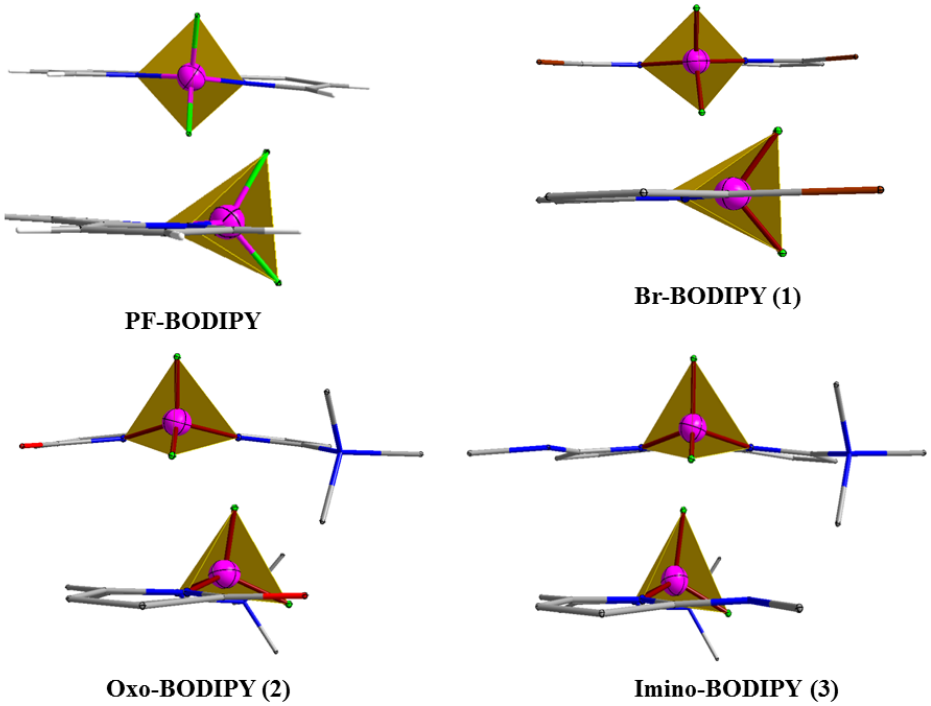

Figure S26. Geometrical arrangement in PF-BODIPY, Br-BODIPY (**1**), Oxo-BODIPY (**2**) and Imino-BODIPY (**3**).

Geometrical calculations	τ_4	THC_{D-A} (%)
PF-BODIPY	0.981	99.7%
Br-BODIPY (1)	0.977	99.5%
Oxo-BODIPY (2)	0.978,	99.7%

Imino-BODIPY (3)	0.977	99.6%

Table S5. Geometrical calculations of PF-BODIPY, Br-BODIPY (**1**), Oxo-BODIPY (**2**) and Imino-BODIPY (**3**).

6. Plausible Reaction Mechanism

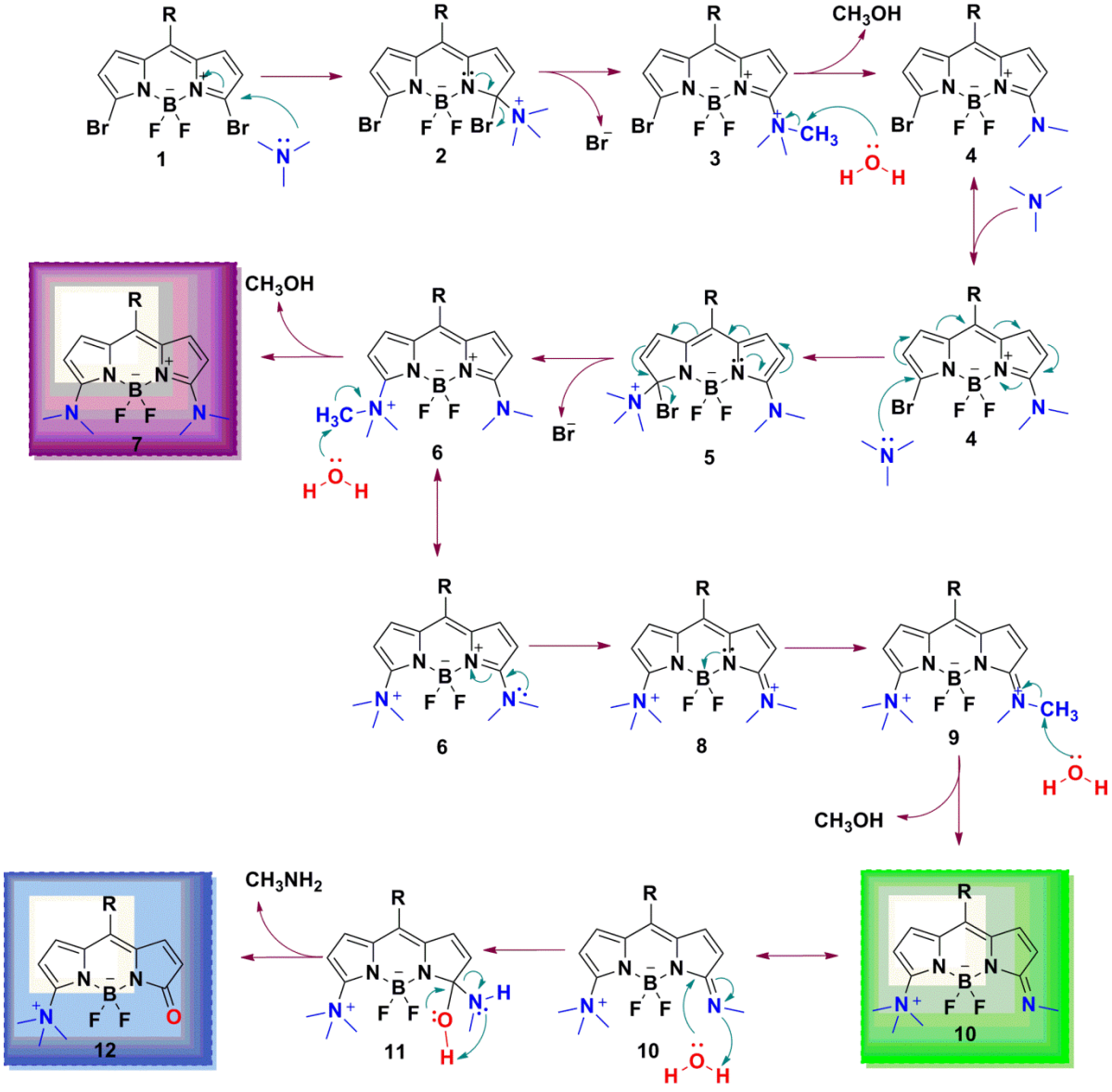

Scheme S2. Plausible reaction mechanism of formation of zwitterionic BODIPYs.

7. Crystallographic information

	Oxo-BODIPY (2)	Imino-BODIPY (3)
Empirical formula	C_{18} H_{13} B F_7 N_3 O	C_{19} H_{16} B F_7 N_4

Formula weight	431.12	444.17
Temperature	110 K	186 K
Wavelength	0.71073	0.71073
Crystal system	Monoclinic	Monoclinic
Space group	P 2(1)/c	P 2(1)/c
Unit cell dimensions	a=15.2794(4)	a=15.712(5)
	b=9.0171(2)	b=9.184(3)
	c=13.5025(4)	c=13.544(4)
	α=90	α=90
	β=111.891(1)	β=111.297(8)
	γ=90	γ=90
Volume	1726.18(8)	1820.9(10)
Z	4	4
Dcalc (g/cm5)	1.659	1.620
Absorption coefficient	0.174	0.160
F(000)	872.0	904.0
T_{min} and T_{max}	0.923, 0.957	0.950, 0.959
Reflections collected	6299	4510
Independent reflections	5298	1646
Goodness-of-fit on F2	1.051	0.960
Final R indices [I>2sigma(I)]	0.0373	0.0645
R indices (all data)	0.1079	0.1699
Largest diff. peak and hole	0.518, -0.246	0.214, -0.335

Table S6. Important crystallographic information of Oxo-BODIPY (**2**) and Imino-BODIPY (**3**).

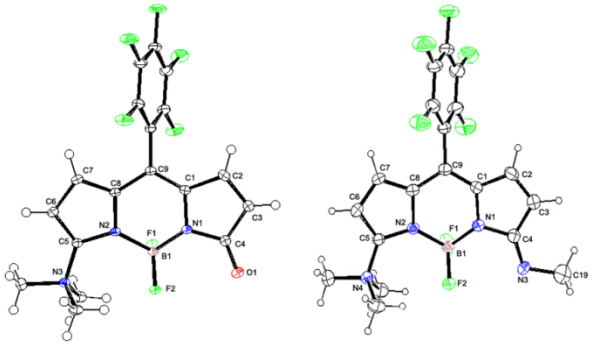

Figure S27. Crystal structures of **a.** Oxo-BODIPY (**2**), **b.** Imino-BODIPY (**3**).

Oxo- BODIPY (2)				**Imino- BODIPY (3)**			
Number	**Atom1**	**Atom2**	**Length**	**Number**	**Atom1**	**Atom2**	**Length**

1	F2	B1	1.381(1)	**1**	F2	B1	1.376(6)
2	F1	B1	1.405(1)	**2**	F1	B1	1.400(5)
3	N2	C8	1.397(1)	**3**	N2	C8	1.401(5)
4	N2	C5	1.381(1)	**4**	N2	C5	1.380(3)
5	N2	B1	1.580(1)	**5**	N2	B1	1.579(4)
6	N1	C1	1.389(1)	**6**	N1	C1	1.388(5)
7	N1	C4	1.393(1)	**7**	N1	C4	1.409(4)
8	N1	B1	1.527(1)	**8**	N1	B1	1.503(5)
9	O1	C4	1.225(2)	**9**	N4	C5	1.477(5)
10	N3	C5	1.473(1)	**10**	N3	C4	1.261(5)
11	C6	C5	1.380(1)	**11**	C8	C9	1.447(4)
12	C6	C7	1.409(2)	**12**	C8	C7	1.374(3)
13	C9	C8	1.443(1)	**13**	C5	C6	1.364(4)
14	C9	C1	1.361(1)	**14**	C9	C10	1.480(5)
15	C8	C7	1.386(1)	**15**	C9	C1	1.348(4)
16	C1	C2	1.451(1)	**16**	C1	C2	1.432(4)
17	C2	C3	1.346(2)	**17**	C4	C3	1.464(5)
18	C4	C3	1.485(2)	**18**	C7	C6	1.384(5)
				19	C2	C3	1.324(6)

Table S7. Important bond lengths in indacene crystal frame work of Oxo-BODIPY (**2**) and Imino-BODIPY (**3**).

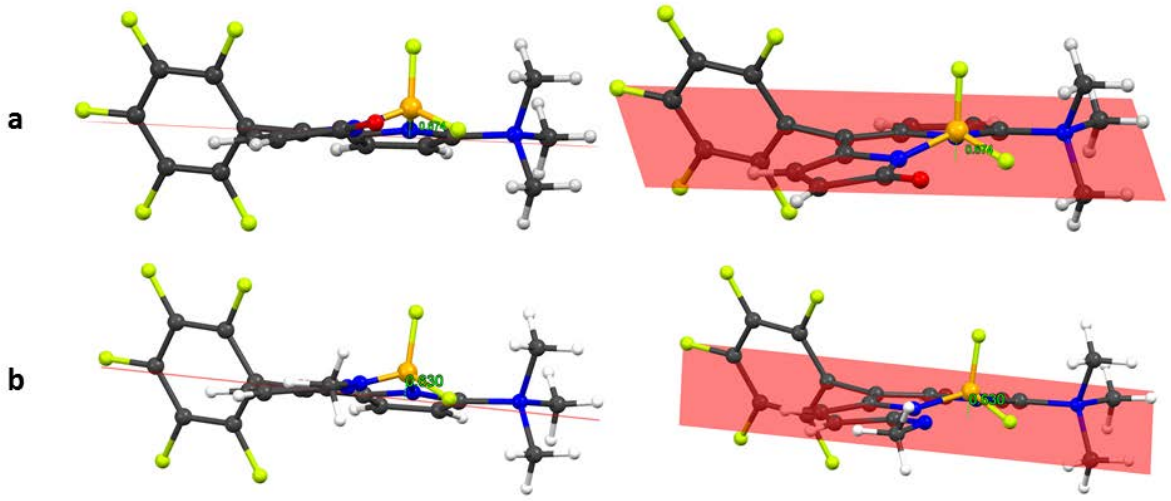

Figure S28. Boron atom displacement from indacene mean plane a). Oxo-BODIPY (**2**), b). Imino-BODIPY (**3**).

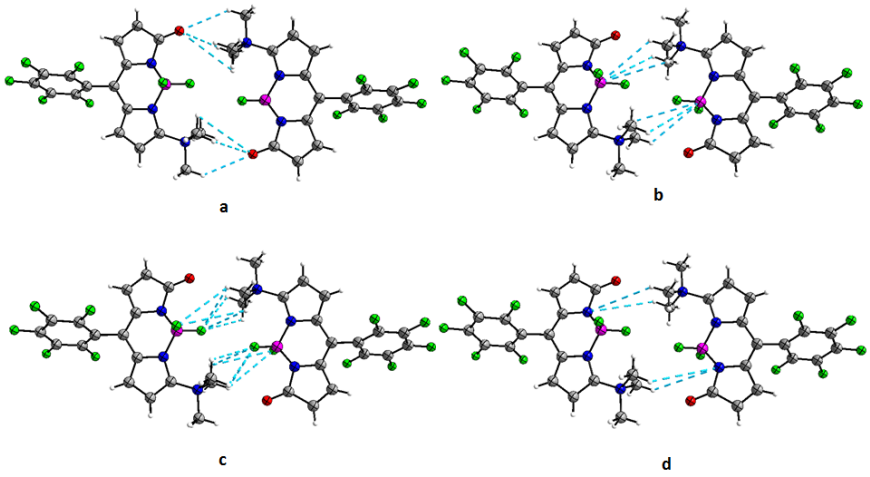

Figure S29. Intermolecular hydrogen bonds in Oxo-BODIPY by a). Oxygen atom, b). Boron atom, c). Fluorine atom and d). Nitrogen atom.

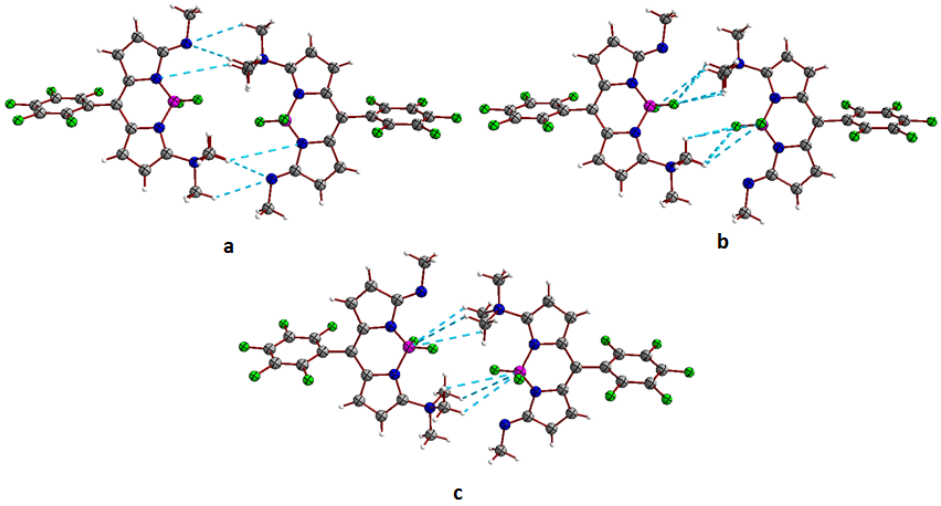

Figure S30. Intermolecular hydrogen bonds in Imino-BODIPY by a). Nitrogen atom, b). Fluorine atom and c). Boron atom.

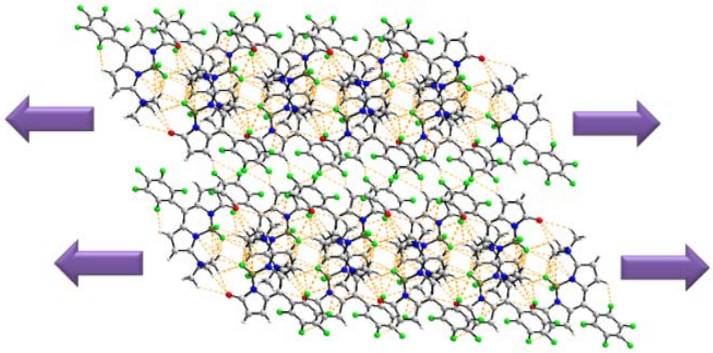

Figure S31. 1-D molecular chain formation by hydrogen bond in crystal frame work of Oxo-BODIPY (**2**).

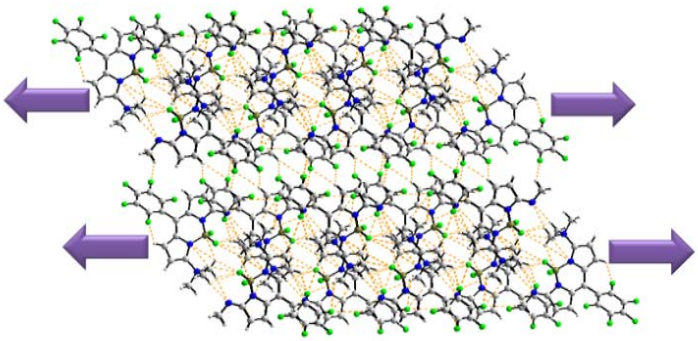

Figure S32. 1-D molecular chain formation by hydrogen bond in crystal frame work of Imino-BODIPY (**3**)

8. Bio- Imaging and toxicity studies

Materials and Method

Yeast Strain and Growth Conditions- Yeast strain used in this study were gifted by Sten Stymne's laboratory; the strains were grown in synthetic complete medium at 25 °C. Genotypes of the strains used in this study are listed on table.1.

Transformations: The WT strain was transformed with the Dcp2pRFP construct using the lithium acetate (LioAC) transformation method (Brachmann *et al.*, 1998)[3]. For selection of positive colonies, transformants were plated onto dropout media (without Leucine).

Strain	Genotype	Reference[4]
SCY62	MATa ADE2	Sandager et al.2002
H1246	MATα are1-Δ::HIS3 are2-Δ::LEU2 dga1-Δ::KanMX4 lro1-Δ::TRP1 ADE2	Sandager et al.2002
yRP1825	MAT_ leu2-3,112 trp1 ura3-52 his4-539 DCP2-GFP (NEO)	Teixeira et al, 2005

Table S8. Genotypes of yeast strains which used in fluorescence imaging.

Fluorescence microscopy

Yeast strains were grown at 25 °C in synthetic complete medium and harvested at OD 0.8, subsequently washed twice with PBS and re-suspended in PBS. Fluorescence imaging was performed as described previously (Madeira et al. 2015). 1 µl of 10 mM BODIPY (BODIPY493/506, IminoBODIPY434/506 (**3**) and Oxo-BODIPY390/405 (**2**)) and 2 µl of vector mounting media were added on 2 µl of yeast cells and fluorescence images were captured with ZEISS Axio ImagerM2 Apotome.2 on 63X oil immersion objective lens.

Commercial available BODIPY 493-506 –Difluoro {2-[1-(3, 5-dimethyl-2H-pyrrol-2-ylidene-N) ethyl]-3, 5-dimethyl-1H-pyrrolato-N}boron which is specifically bind to lipid droplets purchased from Sigma-Aldrich used to test lipids presence in mutant Quadruple yeast cells.[7]

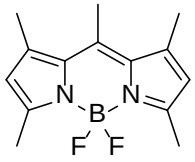

BODIPY 493-506

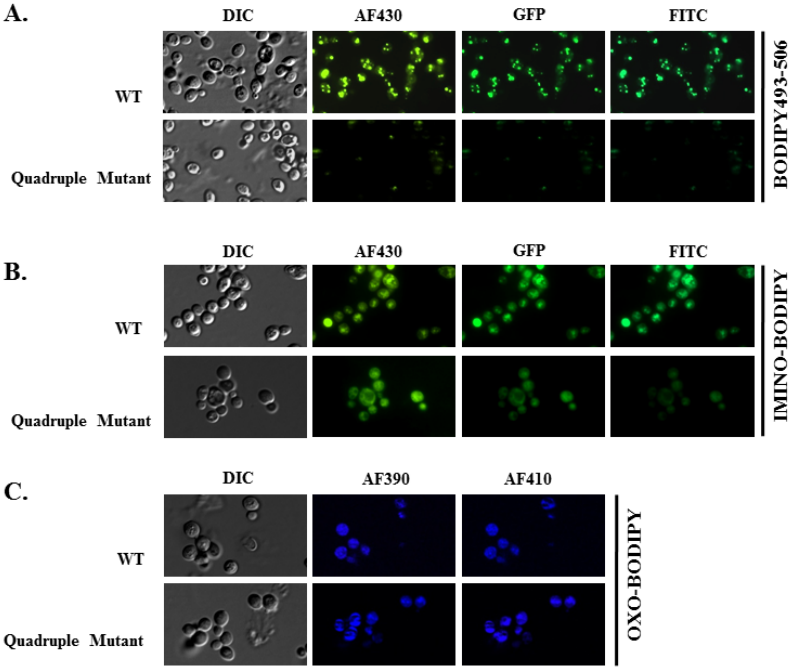

Figure S33. Fluorescence emission imaging of (**A**) BODIPY 493-506, (**B**) Imino-BODIPY (**3**) and (**C**) OXO-BODIPY (**2**) on wild-type yeast strain (SCY62) and mutant (H1246 -Quadruple Mutant).

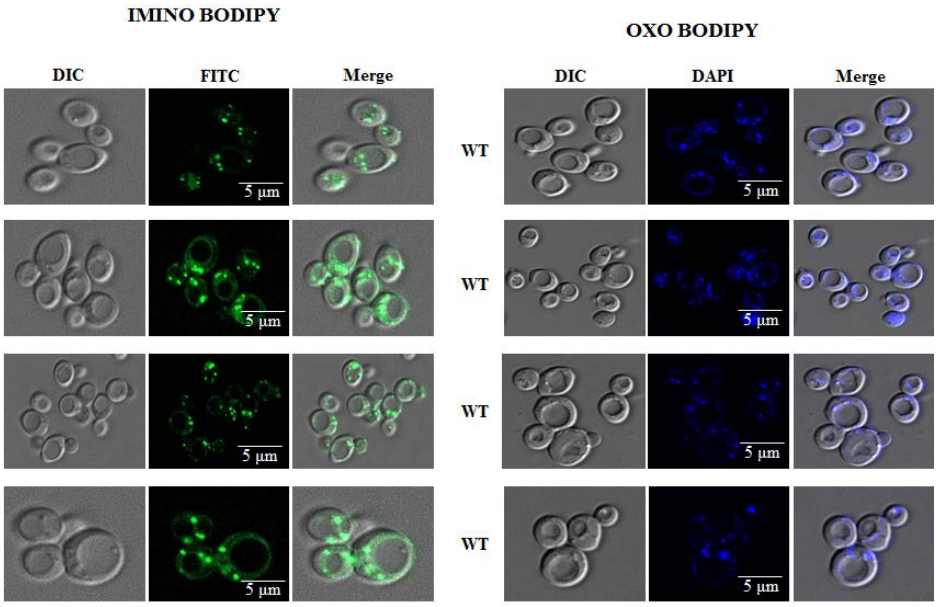

Figure S34. Fluorescence imaging of Imino-BODIPY (**3**) and OXO-BODIPY (**2**) on yeast strain (SCY62).

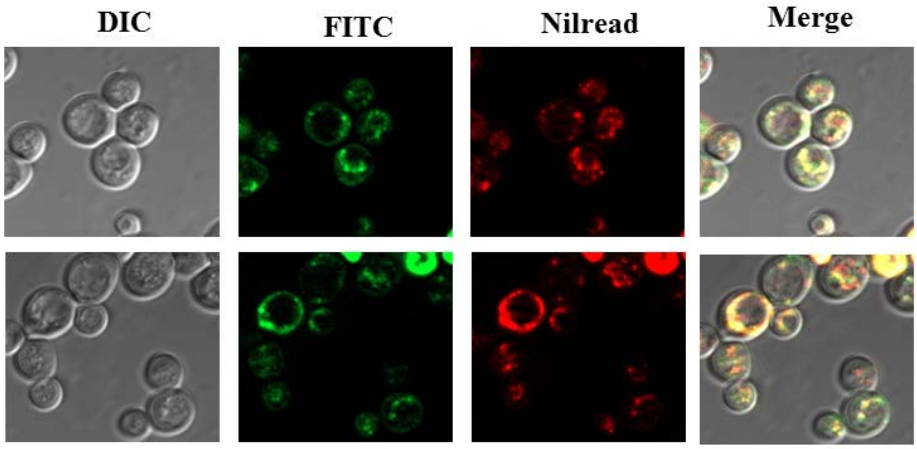

Figure S35. Comparison of fluorescence imaging with Imino-BODIPY (**3**) and Dcp2pRFP transformed SCY62 yeast strain.

Growth Curve Assay: The strain taken for this study was BY4741 (MATa his3Δ1 leu2Δ0 met15Δ0 ura3Δ0). The cells were grown overnight in synthetic complete media (Synthetic Complete Media: YNB 0.17%, Amino Acids 0.18%, Ammonium Sulphate 0.5%, Glucose 2%), then inoculated secondary at OD_{600} 0.2 and allowed to grow till exponential phase (OD_{600} 0.8). Cells growing in exponential phase were normalized to OD_{600} 0.1 in each well of 96 well plate and treated with fluorescent dyes BODIPY493/503, Imino-BODIPY, Oxo-BODIPY. The cells were incubated in plate reader at 30^{o}C for 19 hours where OD_{600} reading was taken at every 30 minutes time interval.

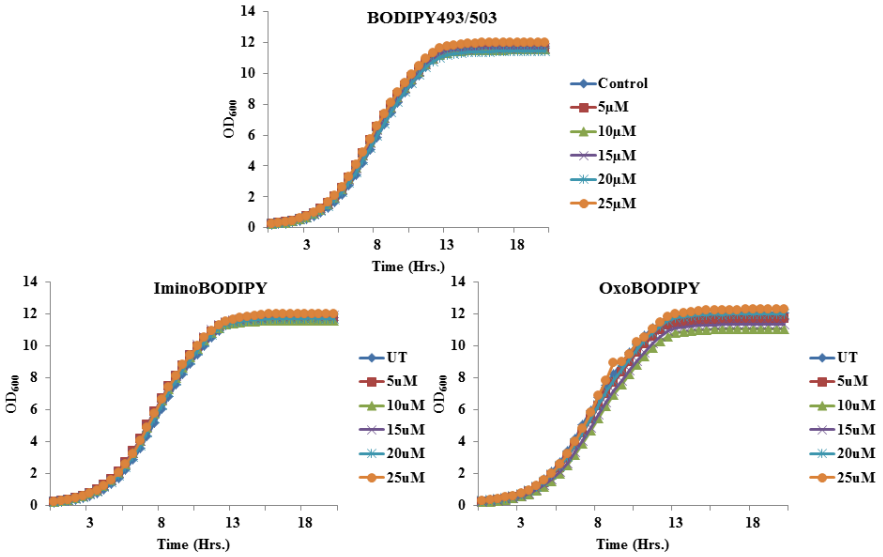

Figure S36. Growth curve assay of Commercial BODIPY493/503, Oxo-BODIPY (**2**) and Imino-BODIPY (**3**) up to 25 μM concentration of dye.

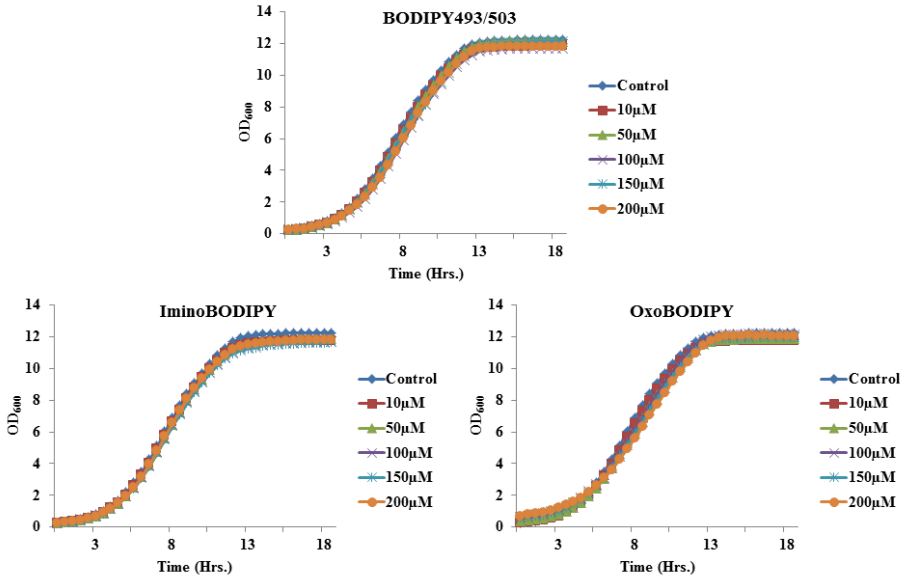

Figure S37. Growth curve assay of Commercial BODIPY493/503, Oxo-BODIPY (**2**) and Imino-BODIPY (**3**) up to 200 μM concentration of dye.

9. Computational calculation

In order to support the optical properties and zwitterionic nature of BODIPYs, we carried out time-dependent density functional theory (TD-DFT/PCM) calculations at B3LYP/6-31G (d) level using Gaussian 09 suite of programs.14 Structural coordinates obtained from crystal data were used for single point energy calculations.

The highest occupied molecular orbital (HOMO) energy of oxo-BODIPY is slightly stabilized than the imino-BODIPY. This may be due to the higher electronegativity of oxygen. The lowest occupied molecular orbital (LUMO) of zwitterionic BODIPYs lie predominantly on the weakly delocalized pyrrole, but HOMO are spread all over the indacene core. TD-DFT predicted absorption spectra and oscillator transitions support the experimental data. The highest oscillator strength represented the transition from HOMO to LUMO that is similar to S0 → S1 electronic transition; second highest oscillator strength from the contribution of HOMO to LUMO +1 stems from S0 → S2.

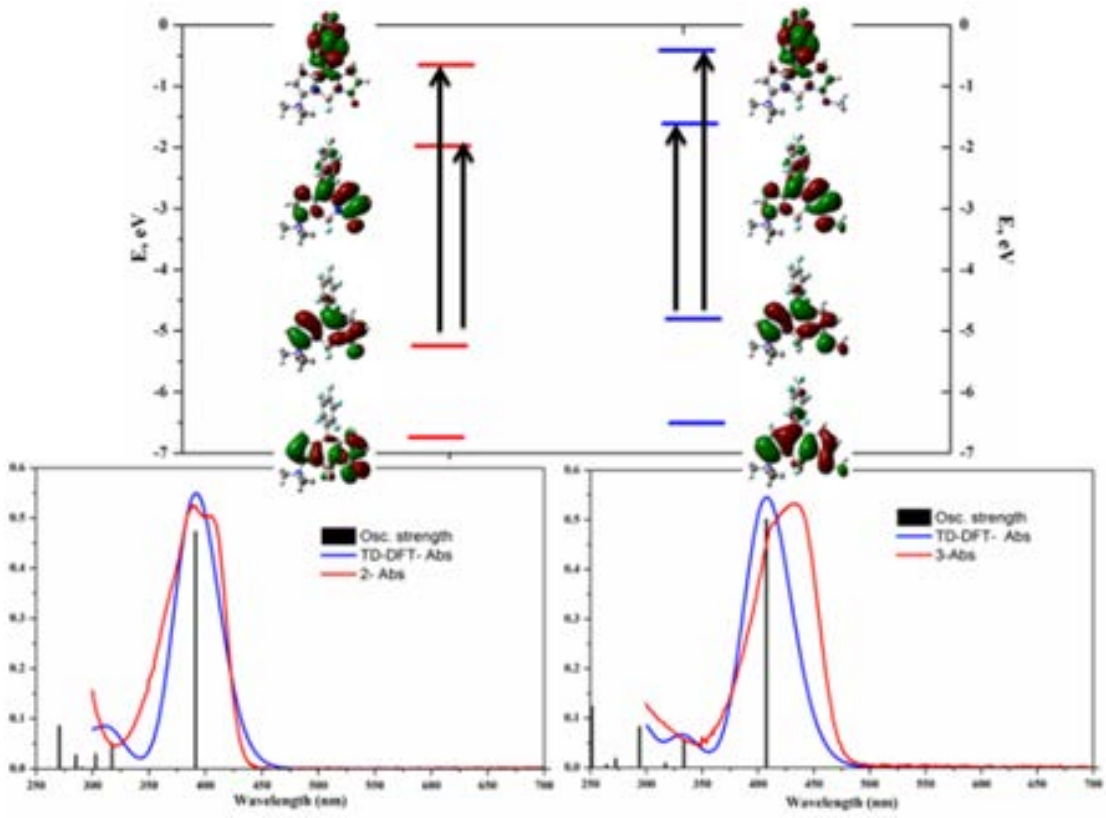

Figure S38. Frontier molecular orbitals and energy levels (above), experimental, predicted TD-DFT absorption spectra and oscillator strength (below) of 2 and 3 in methanol.

Oxo-BODIPY (2)

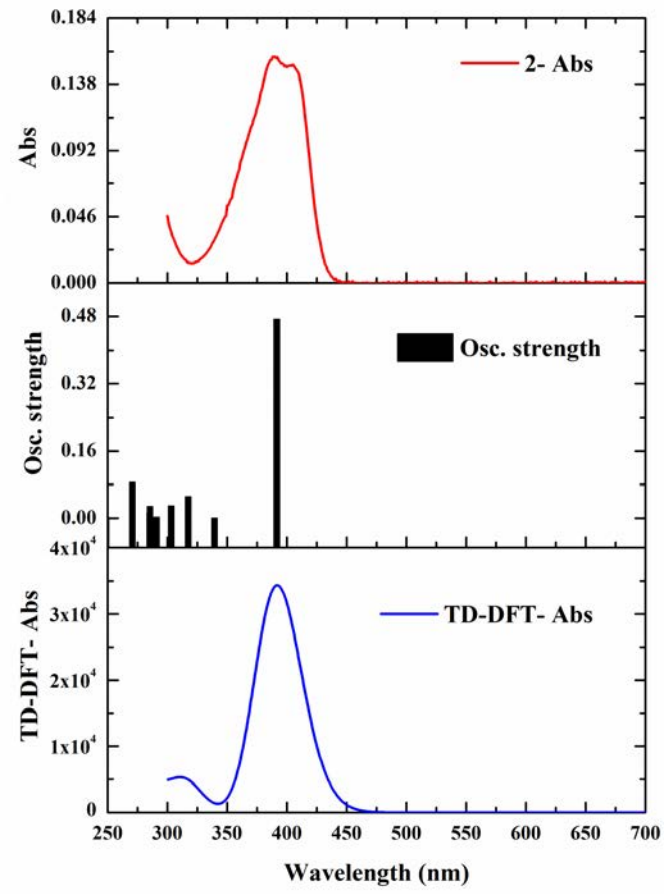

Figure S39. Experimental (top) Oscillator strength (middle) and PCM-TDDFT calculated (bottom) UV-vis spectra of Oxo-BODIPY (**2**) in methanol.

PCM-TDDFT expansion coefficients for Oxo-BODIPY (2)[5]

Excited State 1: Singlet-A 3.1674 eV 391.44 nm f=0.4738 <S**2>=0.000

109 ->110 0.70267

This state for optimization and/or second-order correction.

Total Energy, E(TD-HF/TD-KS) = -1656.79773072

Copying the excited state density for this state as the 1-particle RhoCI density.

Excited State 2: Singlet-A 3.6536 eV 339.34 nm f=0.0006 <S**2>=0.000

107 ->110 0.35475

108 ->110 0.60265

Excited State 3: Singlet-A 3.9073 eV 317.31 nm f=0.0516 <S**2>=0.000

109 ->111 0.70161

Excited State 4: Singlet-A 4.0914 eV 303.04 nm f=0.0302 <S**2>=0.000

104 ->110 -0.15765

106 ->110 -0.14786

107 ->110 0.57509

108 ->110 -0.32907

Excited State 5: Singlet-A 4.2636 eV 290.80 nm f=0.0032 <S**2>=0.000

105 ->110 -0.15710

109 ->112 0.67965

Excited State 6: Singlet-A 4.3450 eV 285.35 nm f=0.0286 <S**2>=0.000

105 ->110 0.44064

106 ->110 0.50663

109 ->112 0.17558

Excited State 7: Singlet-A 4.3479 eV 285.16 nm f=0.0129 <S**2>=0.000

105 ->110 0.52080

106 ->110 -0.43200

107 ->110 -0.13671

Excited State 8: Singlet-A 4.5815 eV 270.62 nm f=0.0862 <S**2>=0.000

103 ->110 0.11217

104 ->110 0.67098

107 ->110 0.10476

Excited State 9: Singlet-A 4.9907 eV 248.43 nm f=0.0028 <S**2>=0.000

103 ->110 -0.11150

109 ->113 0.69405

Excited State 10: Singlet-A 5.0780 eV 244.16 nm f=0.0663 <S**2>=0.000

103 ->110 0.57341

109 ->113 0.11965

109 ->114 -0.36082

Imino-BODIPY (3)

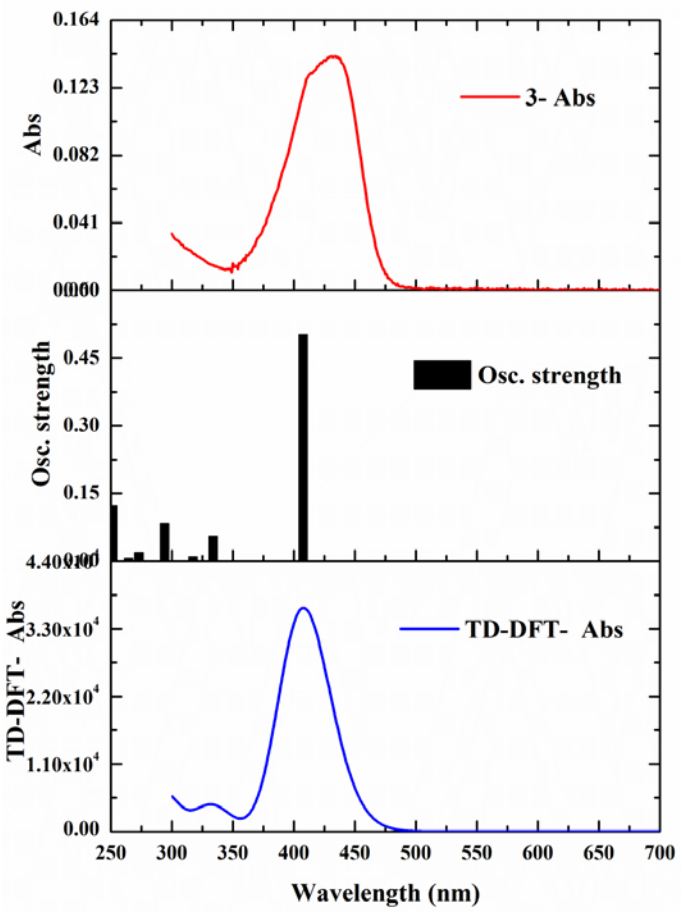

Figure S40. Experimental (top) Oscillator strength (middle) and PCM-TDDFT calculated (bottom) UV-vis spectra of Imino-BODIPY (**3**) in methanol.

PCM-TDDFT expansion coefficients for Imino-BODIPY (3)[5]

Excited State 1: Singlet-A 3.0432 eV 407.42 nm f=0.5020 <S**2>=0.000

113 ->114 0.70136

This state for optimization and/or second-order correction.

Total Energy, E (TD-HF/TD-KS) = -1676.09862012

Copying the excited state density for this state as the 1-particle RhoCI density.

Excited State 2: Singlet-A 3.7155 eV 333.70 nm f=0.0552 <S**2>=0.000

113 ->115 0.70081

Excited State 3: Singlet-A 3.9089 eV 317.19 nm f=0.0097 <S**2>=0.000

113 ->116 0.70460

Excited State 4: Singlet-A 3.9430 eV 314.44 nm f=0.0009 <S**2>=0.000

110 ->114 0.11820

111 ->114 0.69023

Excited State 5: Singlet-A 4.2177 eV 293.96 nm f=0.0833 <S**2>=0.000

108 ->114 -0.12621

112 ->114 0.67483

Excited State 6: Singlet-A 4.4431 eV 279.05 nm f=0.0007 <S**2>=0.000

113 ->117 0.70404

Excited State 7: Singlet-A 4.5451 eV 272.79 nm f=0.0193 <S**2>=0.000

110 ->114 0.68259

111 ->114 -0.12343

Excited State 8: Singlet-A 4.6889 eV 264.42 nm f=0.0068 <S**2>=0.000

109 ->114 0.70191

Excited State 9: Singlet-A 4.9339 eV 251.29 nm f=0.1238 <S**2>=0.000

108 ->114 0.61062

113 ->118 -0.32160

Excited State 10: Singlet-A 5.1127 eV 242.50 nm f=0.0992 <S**2>=0.000

107 ->114 0.51499

108 ->114 -0.15400

113 ->118 -0.44466

10. References

1. Sheldrick, G. M. SHELXTL Program for the Solution of Crystal of Structures, University of Göttingen, Göttingen, Germany, 1993.
2. Sheldrick, G. M. SHELXL 97, Program for Crystal Structure Refinement, University of Göttingen, Göttingen, Germany, 1997.

3. C. B. Brachmann, A. Davies, G. J. Cost, E. Caputo, J. li, P. Hieter, J. D. Boeke, Designer deletion strains derived from Saccharomyces cerevisiae S288C: a useful set of strains and plasmids for PCR-mediated gene disruption and other applications, *Yeats*, **1998**, *14*, 115-132.

4. (a) Sandager L, Gustavsson MH, Ståhl U, Dahlqvist A, Wiberg E, Banas A, Lenman M, Ronne H, Stymne S. 2002. Storage Lipid Synthesis Is Non-essential in Yeast. *J Biol Chem*. **2002**, *277*, 6478-82. (b) Sorger D, Athenstaedt K, Hrastnik C, Daum G. 2004. A Yeast Strain Lacking Lipid Particles Bears a Defect in Ergosterol Formation. *J Biol Chem*. **2004**, *279*, 31190-31196. (c) Madeira JB, Masuda CA, Maya-Monteiro CM, Matos GS, Montero-Lomelí M, Bozaquel-Morais BL. 2015. TORC1 inhibition induces lipid droplet replenishment in yeast. *Mol Cell Biol* 35, 737–746. (d) D. Teixeira, U. Sheth, M. A. Valencia-Sanchez, M. Brengues, R. Parker, Processing bodies require RNA for assembly and contain nontranslating mRNAs. *RNA*, **2005**, *11*, 371-382.

5. Gaussian 09, Revision A02, M. J. Frisch, G. W. Trucks, H. B. Schlegel, G. E. Scuseria, M. A. Robb, J. R. Cheeseman, G. Scalmani, V. Barone, B. Mennucci, G. A. Petersson, H. Nakatsuji, M. Caricato, X. Li, H. P. Hratchian, A. F. Izmaylov, J. Bloino, G. Zheng, J. L. Sonnenberg, M. Hada, M. Ehara, K. Toyota, R. Fukuda, J. Hasegawa, M. Ishida, T. Nakajima, Y. Honda, O. Kitao, H. Nakai, T. Vreven, J. A. Montgomery, Jr., J. E. Peralta, F. Ogliaro, M. Bearpark, J. J. Heyd, E. Brothers, K. N. Kudin, V. N. Staroverov, R. Kobayashi, J. Normand, K. Raghavachari, A. Rendell, J. C. Burant, S. S. Iyengar, J. Tomasi, M. Cossi, N. Rega, J. M. Millam, M. Klene, J. E. Knox, J. B. Cross, V. Bakken, C. Adamo, J. Jaramillo, R. Gomperts, R. E. Stratmann, O. Yazyev, A. J. Austin, R. Cammi, C. Pomelli, J. W. Ochterski, R. L. Martin, K. Morokuma, V. G. Zakrzewski, G. A. Voth, P. Salvador, J. J. Dannenberg, S. Dapprich, A. D. Daniels, Ö. Farkas, J. B. Foresman, J. V. Ortiz, J. Cioslowski, D. J. Fox, Gaussian, Inc., Wallingford CT, **2009**.